



# Impact of Stress and Material Porosity on Double Boost DC-DC Converter Technology to Enhance Field-Effect Heterotransistors and Heterodiodes Density

Evgeny L. Prankatov

*Nizhny Novgorod State University, 23 Gagarin avenue, Nizhny Novgorod, 603950, Russia.*

*Nizhny Novgorod State Agrotechnical University, 97 Gagarin avenue, Nizhny Novgorod, 603950, Russia.*

*elp2004@mail.ru*

Article Info	Abstract
<b>Article history:</b>	
Received Nov 26 <sup>th</sup> , 2023	
Revised May 27 <sup>th</sup> , 2024	
Accepted June 28 <sup>th</sup> , 2024	
Published June 30 <sup>th</sup> , 2024	
<b>Index Terms:</b>	
Heterotransistors	
Double boost DC-DC converters	
Optimization of Manufacturing Prognosis	
	<p>Currently, several critical issues in solid-state electronics, such as improving the performance, reliability and density of integrated circuits elements like diodes, field-effect transistors, and bipolar transistors are being intensively addressed. One effective approach to reduce the dimensions of integrated circuits elements is to manufacture them in thin film heterostructures with an optimal manufacturing regime. In this paper, we explore methods to increase the density of field-effect heterotransistors and heterodiodes in the framework of a double boost DC-DC converter. We consider manufacturing this converter in a heterostructure with a specific configuration, where several required areas of the heterostructure should be doped by diffusion or ion implantation. Subsequently, the dopant and radiation defects should be annealed using an optimized scheme. Based on this approach, we provide recommendations for determining the optimal annealing time to achieve the best compromise between increasing density of integrated circuits elements and minimizing local overheating during their operation. We also propose a method to reduce the mismatch-induced stress in the heterostructure. We present an analytical approach to analyze mass and heat transport in heterostructures during the manufacturing of integrated circuits, accounting for mismatch-induced stress. This approach allows for the consideration of spatial and temporal variations in the parameters of technological processes, as well as their nonlinearity.</p>

## I. INTRODUCTION

At present, several significant problems in solid-state electronics, such as increasing the performance, reliability and density of integrated circuit elements (diodes, field-effect and bipolar transistors), are intensively addressed [1-6]. To increase the performance of these devices, there is a growing interest in identifying materials with higher values of charge carrier mobility [7]-[10]. One method to reduce the dimensions of integrated circuit elements is by manufacturing them in thin film heterostructures [3]-[5][11]. This approach allows for the use of heterostructure inhomogeneity, optimization of doping in electronic materials [12], and the development of epitaxial technology to improve these materials, including analyzing mismatch-induced stress [13]-[15]. Alternative approaches to increase the dimensions of integrated circuits include laser and microwave annealing [16]-[18].

In this paper, we introduce an approach to optimize the manufacture of field-effect *p*-channel MOSFETs and heterodiodes. This approach aims to reduce their dimensions while increasing their density in a double boost DC-DC

converter framework. We also explore methods to minimize mismatch-induced stress to reduce the number of defects generated by this stress. We examine a heterostructure consisting of a substrate, an epitaxial layer and a buffer layer between them (see Figure 1). The epitaxial layer comprises several sections made from different materials, which are doped by diffusion or ion implantation to achieve the required types of conductivity (*p* or *n*). These areas form the sources, drains and gates (see Figure 1). After doping, it is necessary to anneal the dopant and/or radiation defects.

The main aim of this paper is to analyze the redistribution of dopant and radiation defects to determine conditions that allow for the reduction in size of the considered filter elements while simultaneously increasing their density. Additionally, we explore the possibility of reducing mismatch-induced stress in the heterostructure. Based on our analysis, we obtain dependencies of optimal annealing time on several parameters. The optimal annealing time aims to achieve a maximal compromise between increasing the integration rate of the double boost DC-DC converter by reducing element dimension and minimizing local overheating during operation of converter elements by improving the homogeneity of dopant distribution in the

required area. We also propose an approach to reduce mismatch-induced stress in the heterostructure by using a porous buffer layer. An analytical approach to analyze mass and heat transport in heterostructures during manufacturing of integrated circuits with account mismatch-induced stress is

also presented. The approach accounts for spatial and temporal variations in the parameters of technological processes as well as their nonlinearity.

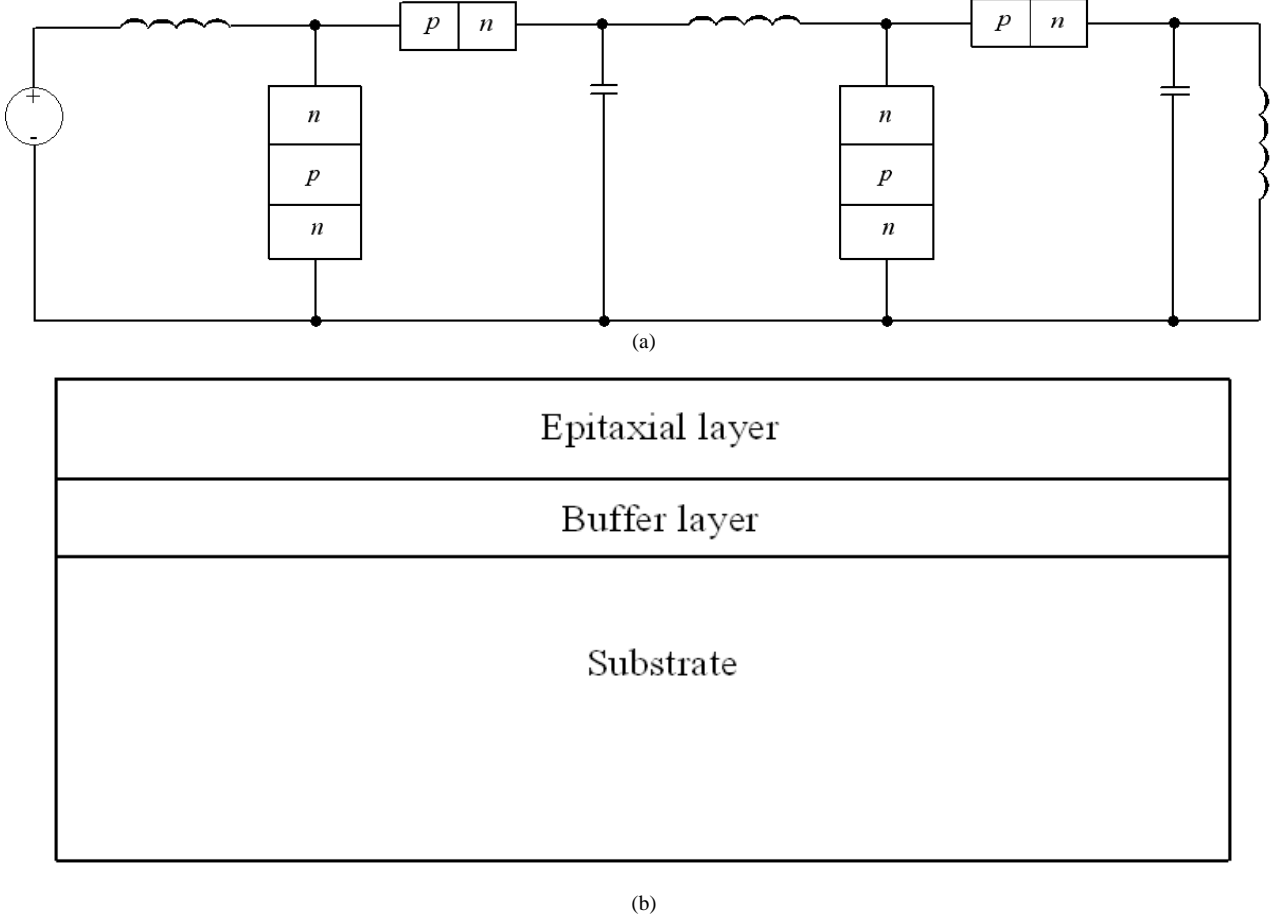


Figure 1. (a) Structure of considered double boost DC-DC converter [1]. (b) Heterostructure with substrate epitaxial layers and buffer layers (side view).

## II. METHOD OF SOLUTION

To achieve the aim of this study, calculation and analysis on the spatio-temporal distribution of the concentration of the

dopant in the heterostructure under consideration. This distribution is determined by solving the second Fick's law, as shown in Equation (1) [1][19]-[23].

$$\begin{aligned} \frac{\partial C(x,y,z,t)}{\partial t} = & \frac{\partial}{\partial x} \left[ D \frac{\partial C(x,y,z,t)}{\partial x} \right] + \frac{\partial}{\partial y} \left[ D \frac{\partial C(x,y,z,t)}{\partial y} \right] + \frac{\partial}{\partial z} \left[ D \frac{\partial C(x,y,z,t)}{\partial z} \right] + \Omega \frac{\partial}{\partial x} \left[ \frac{D_s}{kT} \nabla_s \mu_1(x,y,z,t) \int_0^{L_z} C(x,y,W,t) dW \right] \\ & + \Omega \frac{\partial}{\partial y} \left[ \frac{D_s}{kT} \nabla_s \mu_1(x,y,z,t) \int_0^{L_z} C(x,y,W,t) dW \right] + \frac{\partial}{\partial \vec{x}} x \left[ \frac{D_{CS}}{V k T} \frac{\partial \mu_2(x,y,z,t)}{\partial x} \right] + \frac{\partial}{\partial \vec{x}} y \left[ \frac{D_{CS}}{V k T} \frac{\partial \mu_2(x,y,z,t)}{\partial y} \right] \\ & + \frac{\partial}{\partial \vec{x}} z \left[ \frac{D_{CS}}{V k T} \frac{\partial \mu_2(x,y,z,t)}{\partial z} \right] \end{aligned} \quad (1)$$

with boundary and initial conditions as in Equation (2)

$$\begin{aligned} \left. \frac{\partial C(x,y,z,t)}{\partial x} \right|_{x=0} &= 0, \quad \left. \frac{\partial C(x,y,z,t)}{\partial x} \right|_{x=L_x} = 0 \\ \left. \frac{\partial C(x,y,z,t)}{\partial y} \right|_{y=0} &= 0, \quad \left. \frac{\partial C(x,y,z,t)}{\partial y} \right|_{y=L_y} = 0 \\ \left. \frac{\partial C(x,y,z,t)}{\partial z} \right|_{z=0} &= 0, \quad \left. \frac{\partial C(x,y,z,t)}{\partial z} \right|_{z=L_z} = 0 \\ C(x,y,z,0) &= f_C(x,y,z). \end{aligned} \quad (2)$$

Here  $C(x,y,z,t)$  represents the spatio-temporal distribution of the dopant concentration;  $\Omega$  denotes the atomic volume of the dopant;  $\nabla_s$  is the symbol for the surficial gradient;  $+/-$  is the surficial concentration of the dopant at the interface between the layers of the heterostructure (assuming that the Z-axis is perpendicular to the interface between the layers of heterostructure);  $\mu_1(x,y,z,t)$  and  $\mu_2(x,y,z,t)$  represent the chemical potential due to the presence of mismatch-induced stress and material porosity, respectively;  $D$  and  $D_s$  are the coefficients of volumetric and surficial diffusion. The values of dopant diffusions coefficients depend on the properties of

the heterostructure materials, the rate of heating and cooling during annealing, and the spatio-temporal distribution of the dopant concentration. The dependence of the dopant

$$D_S = D_{SL}(x, y, z, T) \left[ 1 + \xi_S \frac{C^\gamma(x, y, z, t)}{Pr(x, y, z, T)} \right] \left[ 1 + \varsigma_1 \frac{V(x, y, z, t)}{V^*} + \varsigma_2 \frac{V^2(x, y, z, t)}{(V^*)^2} \right] \quad (3)$$

Here  $D_L(x, y, z, T)$  and  $D_{LS}(x, y, z, T)$  represent the spatial (accounting for all layers of heterostructure) and temperature (due to Arrhenius law) dependences of the dopant diffusion coefficients, respectively;  $T$  is the annealing temperature and  $P(x, y, z, T)$  is the solubility limit of the dopant. The parameter  $\gamma$  depends on the properties of the materials and can be an integer in the interval  $\gamma \in [1][3][24]$ .  $V(x, y, z, t)$  denotes the spatio-temporal distribution of the concentration of radiation

$$\begin{aligned} \frac{\partial I(x, y, z, t)}{\partial t} &= \frac{\partial}{\partial x} \left[ D_I(x, y, z, T) \frac{\partial I(x, y, z, t)}{\partial x} \right] + \frac{\partial}{\partial y} \left[ D_I(x, y, z, T) \frac{\partial I(x, y, z, t)}{\partial y} \right] + \frac{\partial}{\partial z} \left[ D_I(x, y, z, T) \frac{\partial I(x, y, z, t)}{\partial z} \right] - k_{I,V}(x, y, z, T) I^2(x, y, z, t) \\ &\quad - k_{I,V}(x, y, z, T) \times I(x, y, z, t) V(x, y, z, t) + \Omega \frac{\partial}{\partial x} \left[ \frac{D_{IS}}{kT} \nabla_S \mu(x, y, z, t) \int_0^{L_z} I(x, y, W, t) dW \right] \\ &\quad + \Omega \frac{\partial}{\partial y} \left[ \frac{D_{IS}}{kT} \nabla_S \mu(x, y, z, t) \int_0^{L_z} I(x, y, W, t) dW \right] + \frac{\partial}{\partial x} \left[ \frac{D_{IS}}{\bar{V}kT} \frac{\partial \mu_2(x, y, z, t)}{\partial x} \right] + \frac{\partial}{\partial y} \left[ \frac{D_{IS}}{\bar{V}kT} \frac{\partial \mu_2(x, y, z, t)}{\partial y} \right] \\ &\quad + \frac{\partial}{\partial z} \left[ \frac{D_{IS}}{\bar{V}kT} \frac{\partial \mu_2(x, y, z, t)}{\partial z} \right] + \frac{\partial V(x, y, z, t)}{\partial t} \\ &= \frac{\partial}{\partial x} \left[ D_V(x, y, z, T) \frac{\partial V(x, y, z, t)}{\partial x} \right] + \frac{\partial}{\partial y} \left[ D_V(x, y, z, T) \frac{\partial V(x, y, z, t)}{\partial y} \right] + \frac{\partial}{\partial z} \left[ D_V(x, y, z, T) \frac{\partial V(x, y, z, t)}{\partial z} \right] \\ &\quad - k_{V,V}(x, y, z, T) V^2(x, y, z, t) - k_{I,V}(x, y, z, T) \times I(x, y, z, t) V(x, y, z, t) + \Omega \frac{\partial}{\partial x} \left[ \frac{D_{VS}}{kT} \nabla_S \mu(x, y, z, t) \int_0^{L_z} V(x, y, W, t) dW \right] \\ &\quad + \Omega \frac{\partial}{\partial y} \left[ \frac{D_{VS}}{kT} \nabla_S \mu(x, y, z, t) \int_0^{L_z} V(x, y, W, t) dW \right] + \frac{\partial}{\partial x} \left[ \frac{D_{VS}}{\bar{V}kT} \frac{\partial \mu_2(x, y, z, t)}{\partial x} \right] + \frac{\partial}{\partial y} \left[ \frac{D_{VS}}{\bar{V}kT} \frac{\partial \mu_2(x, y, z, t)}{\partial y} \right] \\ &\quad + \frac{\partial}{\partial z} \left[ \frac{D_{VS}}{\bar{V}kT} \frac{\partial \mu_2(x, y, z, t)}{\partial z} \right] \end{aligned} \quad (4)$$

with boundary and initial conditions as in Equation (5)

$$\begin{aligned} \frac{\partial I(x, y, z, t)}{\partial x} \Big|_{x=0} &= 0, & \frac{\partial I(x, y, z, t)}{\partial x} \Big|_{x=L_x} &= 0 \\ \frac{\partial I(x, y, z, t)}{\partial y} \Big|_{y=0} &= 0, & \frac{\partial I(x, y, z, t)}{\partial y} \Big|_{y=L_y} &= 0 \\ \frac{\partial I(x, y, z, t)}{\partial z} \Big|_{z=0} &= 0, & \frac{\partial I(x, y, z, t)}{\partial z} \Big|_{z=L_z} &= 0 \\ \frac{\partial V(x, y, z, t)}{\partial x} \Big|_{x=0} &= 0, & \frac{\partial V(x, y, z, t)}{\partial x} \Big|_{x=L_x} &= 0 \\ \frac{\partial V(x, y, z, t)}{\partial y} \Big|_{y=0} &= 0, & \frac{\partial V(x, y, z, t)}{\partial y} \Big|_{y=L_y} &= 0 \\ \frac{\partial V(x, y, z, t)}{\partial z} \Big|_{z=0} &= 0, & \frac{\partial V(x, y, z, t)}{\partial z} \Big|_{z=L_z} &= 0 \end{aligned} \quad (5)$$

$$I(x, y, z, 0) = f_I(x, y, z), V(x, y, z, 0) = f_V(x, y, z),$$

$$V(x_1 + V_n t, y_1 + V_n t, z_1 + V_n t, t) = V_\infty \left( 1 + \frac{2\ell\omega}{kT\sqrt{x_1^2 + y_1^2 + z_1^2}} \right)$$

Here,  $I(x, y, z, t)$  represents the spatio-temporal distribution of concentration of radiation interstitials, while  $I^*$  denotes the equilibrium distribution of interstitials. The coefficient of volumetric and surficial diffusions of interstitials and vacancies are given by  $D_I(x, y, z, T)$ ,  $D_V(x, y, z, T)$ ,  $D_{IS}(x, y, z, T)$ ,  $D_{VS}(x, y, z, T)$ , respectively. The terms  $V^2(x, y, z, t)$  and  $I^2(x, y, z, t)$  correspond to the generation of divacancies and

diffusion coefficients on these parameters can be approximated by Equation (3) [24]-[26].

vacancies, while  $V^*$  represents the equilibrium distribution of vacancies. The concentration dependence of the dopant diffusion coefficient has been described in detail in [23]. The spatio-temporal distributions of the concentration of point radiation defects have been determined by solving Equation (4) [1]-[23][25][26]

diinterstitials, respectively (see, for example, [26] and the appropriate references in this book). The parameters  $k_{I,V}(x, y, z, T)$ ,  $k_{I,I}(x, y, z, T)$  and  $k_{V,V}(x, y, z, T)$  describe the recombination of point radiation defects and the generation of their complexes. Here,  $k$  is the Boltzmann constant;  $\omega = a^3$ , where  $a$  is the interatomic distance, and  $\ell$  is the specific surface energy. To account for the porosity of buffer layers, we assume that the pores are approximately cylindrical with average values  $r = \sqrt{x_1^2 + y_1^2}$  and  $z_1$  before annealing [23]. Over time, small pores decompose into vacancies, which are then absorbed by larger pores [27]. As time progresses, the larger pores grow by absorbing the vacancies and became more spherical [27]. The distribution of the concentration of vacancies in the heterostructure, which exists due to porosity, can be determined by summing over all pores, for example

$$V(x, y, z, t) = \sum_{i=0}^l \sum_{j=0}^m \sum_{k=0}^n V_p(x + i\alpha, y + j\beta, z + k\chi, t) \quad (6)$$

$$R = \sqrt{x^2 + y^2 + z^2}$$

Here  $\alpha$ ,  $\beta$  and  $\chi$  are the average distances between the centers of pores in the directions  $x$ ,  $y$  and  $z$ , respectively, and  $l$ ,  $m$  and  $n$  are the quantities of pores the inappropriate directions. The spatio-temporal distributions of divacancies  $\Phi_V(x, y, z, t)$  and diinterstitials  $\Phi_I(x, y, z, t)$  can be determined by solving Equations (7a) and (7b) [25][26]

$$\begin{aligned} \frac{\partial \Phi_I(x, y, z, t)}{\partial t} = & \frac{\partial}{\partial x} \left[ D_{\phi_I}(x, y, z, T) \frac{\partial \Phi_I(x, y, z, t)}{\partial x} \right] + \frac{\partial}{\partial y} \left[ D_{\phi_I}(x, y, z, T) \frac{\partial \Phi_I(x, y, z, t)}{\partial y} \right] + \frac{\partial}{\partial z} \left[ D_{\phi_I}(x, y, z, T) \frac{\partial \Phi_I(x, y, z, t)}{\partial z} \right] \\ & + \Omega \frac{\partial}{\partial x} \left[ \frac{D_{\phi_{IS}}}{kT} V_S \mu_1(x, y, z, t) \int_0^{L_z} \Phi_I(x, y, W, t) dW \right] + \Omega \frac{\partial}{\partial y} \left[ \frac{D_{\phi_{IS}}}{kT} V_S \mu_1(x, y, z, t) \int_0^{L_z} \Phi_I(x, y, W, t) dW \right] \\ & + k_{I,I}(x, y, z, T) I^2(x, y, z, t) + \frac{\partial}{\partial x} \left[ \frac{D_{\phi_{IS}} \partial \mu_2(x, y, z, t)}{\bar{V}kT} \right] + \frac{\partial}{\partial y} \left[ \frac{D_{\phi_{IS}} \partial \mu_2(x, y, z, t)}{\bar{V}kT} \right] + \frac{\partial}{\partial z} \left[ \frac{D_{\phi_{IS}} \partial \mu_2(x, y, z, t)}{\bar{V}kT} \right] \\ & + k_I(x, y, z, T) I(x, y, z, t) \end{aligned} \quad (7a)$$

$$\begin{aligned} \frac{\partial \Phi_V(x, y, z, t)}{\partial t} = & \frac{\partial}{\partial x} \left[ D_{\phi_V}(x, y, z, T) \frac{\partial \Phi_V(x, y, z, t)}{\partial x} \right] + \frac{\partial}{\partial y} \left[ D_{\phi_V}(x, y, z, T) \frac{\partial \Phi_V(x, y, z, t)}{\partial y} \right] + \frac{\partial}{\partial z} \left[ D_{\phi_V}(x, y, z, T) \frac{\partial \Phi_V(x, y, z, t)}{\partial z} \right] \\ & + \Omega \frac{\partial}{\partial x} \left[ \frac{D_{\phi_{VS}}}{kT} V_S \mu_1(x, y, z, t) \int_0^{L_z} \Phi_V(x, y, W, t) dW \right] + \Omega \frac{\partial}{\partial y} \left[ \frac{D_{\phi_{VS}}}{kT} V_S \mu_1(x, y, z, t) \int_0^{L_z} \Phi_V(x, y, W, t) dW \right] \\ & + k_{V,V}(x, y, z, T) V^2(x, y, z, t) + \frac{\partial}{\partial x} \left[ \frac{D_{\phi_{VS}} \partial \mu_2(x, y, z, t)}{\bar{V}kT} \right] + \frac{\partial}{\partial y} \left[ \frac{D_{\phi_{VS}} \partial \mu_2(x, y, z, t)}{\bar{V}kT} \right] + \frac{\partial}{\partial z} \left[ \frac{D_{\phi_{VS}} \partial \mu_2(x, y, z, t)}{\bar{V}kT} \right] \\ & + k_V(x, y, z, T) V(x, y, z, t) \end{aligned} \quad (7b)$$

with boundary and initial conditions as given in Equation (8)

$$\begin{aligned} \frac{\partial \Phi_I(x, y, z, t)}{\partial x} \Big|_{x=0} &= 0, \quad \frac{\partial I(x, y, z, t)}{\partial x} \Big|_{x=L_x} = 0 \\ \frac{\partial I(x, y, z, t)}{\partial y} \Big|_{y=0} &= 0, \quad \frac{\partial I(x, y, z, t)}{\partial y} \Big|_{y=L_y} = 0 \\ \frac{\partial \Phi_I(x, y, z, t)}{\partial z} \Big|_{z=0} &= 0, \quad \frac{\partial I(x, y, z, t)}{\partial z} \Big|_{z=L_z} = 0 \\ \frac{\partial \Phi_V(x, y, z, t)}{\partial x} \Big|_{x=0} &= 0, \quad \frac{\partial V(x, y, z, t)}{\partial x} \Big|_{x=L_x} = 0 \\ \frac{\partial V(x, y, z, t)}{\partial y} \Big|_{y=0} &= 0, \quad \frac{\partial V(x, y, z, t)}{\partial y} \Big|_{y=L_y} = 0 \\ \frac{\partial V(x, y, z, t)}{\partial z} \Big|_{z=0} &= 0, \quad \frac{\partial V(x, y, z, t)}{\partial z} \Big|_{z=L_z} = 0 \\ \Phi_I(x, y, z, 0) &= f_{\Phi_I}(x, y, z), \quad \Phi_V(x, y, z, 0) = f_{\Phi_V}(x, y, z) \end{aligned} \quad (8)$$

Here,  $D_{\phi_I}(x, y, z, T)$ ,  $D_{\phi_V}(x, y, z, T)$ ,  $D_{\phi_{IS}}(x, y, z, T)$  and  $D_{\phi_{VS}}(x, y, z, T)$  are the coefficients of volumetric and surficial diffusions of radiation defects complexes. The parameters  $k_I(x, y, z, T)$  and  $k_V(x, y, z, T)$  describe the decay of the radiation defects complexes.

The chemical potential  $\mu_1$  in Equation (1) can be determined using the relation in Equation (9) [19],

$$\mu_1 = E(z) \Omega \sigma_{ij} [u_{ij}(x, y, z, t) + u_{ji}(x, y, z, t)] / 2 \quad (9)$$

where  $E(z)$  is the Young's modulus,  $\sigma_{ij}$  is the stress tensor, and  $u_{ij} = \frac{1}{2} \left( \frac{\partial u_i}{\partial x_j} + \frac{\partial u_j}{\partial x_i} \right)$  is the deformation tensor. Here,  $u_i$  and  $u_j$  are the components  $u_x(x, y, z, t)$ ,  $u_y(x, y, z, t)$ , and  $u_z(x, y, z, t)$  of the displacement vector  $\vec{u}(x, y, z, t)$ , and  $x_i$  and  $x_j$  are the coordinate  $x$ ,  $y$ ,  $z$ . Equation (4) can be transformed to the Equation (10), where  $\sigma$  is the Poisson coefficient,  $\varepsilon_0 = (a_s - a_{EL})/a_{EL}$  is the mismatch parameter,  $a_s$  and  $a_{EL}$  are the lattice distances of the substrate and the epitaxial layer,  $K$  is the modulus of uniform compression,  $\beta$  is the coefficient of thermal expansion, and  $T_r$  is the equilibrium temperature, which coincides with room temperature in our case. The

$$\begin{aligned} \rho(z) \frac{\partial^2 u_x(x, y, z, t)}{\partial t^2} = & \left\{ K(z) + \frac{5E(z)}{6[1 + \sigma(z)]} \right\} \frac{\partial^2 u_x(x, y, z, t)}{\partial x^2} + \left\{ K(z) - \frac{E(z)}{3[1 + \sigma(z)]} \right\} \frac{\partial^2 u_y(x, y, z, t)}{\partial x \partial y} \\ & + \frac{E(z)}{2[1 + \sigma(z)]} \left[ \frac{\partial^2 u_y(x, y, z, t)}{\partial y^2} + \frac{\partial^2 u_z(x, y, z, t)}{\partial z^2} \right] + \left[ K(z) + \frac{E(z)}{3[1 + \sigma(z)]} \right] \frac{\partial^2 u_z(x, y, z, t)}{\partial x \partial z} - K(z) \beta(z) \frac{\partial T(x, y, z, t)}{\partial x} \end{aligned} \quad (12a)$$

$$\begin{aligned} \rho(z) \frac{\partial^2 u_y(x, y, z, t)}{\partial t^2} = & \frac{E(z)}{2[1 + \sigma(z)]} \left[ \frac{\partial^2 u_y(x, y, z, t)}{\partial x^2} + \frac{\partial^2 u_x(x, y, z, t)}{\partial x \partial y} \right] - \frac{\partial T(x, y, z, t)}{\partial y} \times K(z) \beta(z) \\ & + \frac{\partial}{\partial z} \left\{ \frac{E(z)}{2[1 + \sigma(z)]} \left[ \frac{\partial u_y(x, y, z, t)}{\partial z} + \frac{\partial u_z(x, y, z, t)}{\partial y} \right] \right\} + \frac{\partial^2 u_y(x, y, z, t)}{\partial y^2} \times \left\{ \frac{5E(z)}{12[1 + \sigma(z)]} + K(z) \right\} \\ & + \left\{ K(z) - \frac{E(z)}{6[1 + \sigma(z)]} \right\} \frac{\partial^2 u_y(x, y, z, t)}{\partial y \partial z} + K(z) \frac{\partial^2 u_y(x, y, z, t)}{\partial x \partial y} \end{aligned} \quad (12b)$$

components of the displacement vector can be obtained by solving Equations (11a), (11b) and (11c) respectively [20],

$$\begin{aligned} \mu(x, y, z, t) = & \left[ \frac{\partial u_i(x, y, z, t)}{\partial x_j} \right. \\ & + \frac{\partial u_j(x, y, z, t)}{\partial x_i} \left. \right] \left\{ \frac{1}{2} \left[ \frac{\partial u_i(x, y, z, t)}{\partial x_j} \right. \right. \\ & + \frac{\partial u_j(x, y, z, t)}{\partial x_i} \left. \right] - \varepsilon_0 \delta_{ij} \\ & + \frac{\sigma(z) \delta_{ij}}{1 - 2\sigma(z)} \left[ \frac{\partial u_k(x, y, z, t)}{\partial x_k} - 3\varepsilon_0 \right] \\ & - K(z) \beta(z) [T(x, y, z, t) \\ & - T_r] \delta_{ij} \left. \right\} \frac{\Omega}{2} E(z) \end{aligned} \quad (10)$$

$$\rho(z) \frac{\partial^2 u_x(x, y, z, t)}{\partial t^2} = \frac{\partial \sigma_{xx}(x, y, z, t)}{\partial x} + \frac{\partial \sigma_{xy}(x, y, z, t)}{\partial y} \quad (11a)$$

$$\rho(z) \frac{\partial^2 u_y(x, y, z, t)}{\partial t^2} = \frac{\partial \sigma_{yx}(x, y, z, t)}{\partial x} + \frac{\partial \sigma_{yy}(x, y, z, t)}{\partial y} \quad (11b)$$

$$\rho(z) \frac{\partial^2 u_z(x, y, z, t)}{\partial t^2} = \frac{\partial \sigma_{zx}(x, y, z, t)}{\partial x} + \frac{\partial \sigma_{zy}(x, y, z, t)}{\partial y} \quad (11c)$$

where

$$\begin{aligned} \sigma_{ij} = & \frac{E(z)}{2[1 + \sigma(z)]} \left[ \frac{\partial u_i(x, y, z, t)}{\partial x_j} + \frac{\partial u_j(x, y, z, t)}{\partial x_i} \right. \\ & \left. - \frac{\delta_{ij}}{3} \frac{\partial u_k(x, y, z, t)}{\partial x_k} \right] \\ & + K(z) \delta_{ij} \frac{\partial u_k(x, y, z, t)}{\partial x_k} \\ & - \beta(z) K(z) [T(x, y, z, t) - T_r] \end{aligned} \quad (11d)$$

where  $\rho(z)$  is the density of the heterostructure materials, and  $\delta_{ij}$  is the Kronecker delta symbol. Taking into account the relation for  $\sigma_{ij}$ , the last system of equation can be written as Equation (12).

$$\rho(z) \frac{\partial^2 u_z(x, y, z, t)}{\partial t^2} = \frac{E(z)}{2[1 + \sigma(z)]} \left[ \frac{\partial^2 u_z(x, y, z, t)}{\partial x^2} + \frac{\partial^2 u_z(x, y, z, t)}{\partial y^2} + \frac{\partial^2 u_z(x, y, z, t)}{\partial x \partial z} + \frac{\partial^2 u_z(x, y, z, t)}{\partial y \partial z} \right] \\ + \frac{\partial}{\partial z} \left\{ K(z) \left[ \frac{\partial u_x(x, y, z, t)}{\partial x} + \frac{\partial u_y(x, y, z, t)}{\partial y} + \frac{\partial u_z(x, y, z, t)}{\partial z} \right] \right\} \\ + \frac{1}{6} \frac{\partial}{\partial z} \left\{ \frac{E(z)}{1 + \sigma(z)} \left[ 6 \frac{\partial u_z(x, y, z, t)}{\partial z} - \frac{\partial u_x(x, y, z, t)}{\partial x} - \frac{\partial u_y(x, y, z, t)}{\partial y} - \frac{\partial u_z(x, y, z, t)}{\partial z} \right] \right\} - K(z) \beta(z) \frac{\partial T(x, y, z, t)}{\partial z} \quad (12c)$$

The conditions for the system of Equation (12) can be written as shown in Equation (13).

$$\begin{aligned} \frac{\partial \vec{u}(0, y, z, t)}{\partial x} &= 0, & \frac{\partial \vec{u}(L_x, y, z, t)}{\partial x} &= 0 \\ \frac{\partial \vec{u}(x, 0, z, t)}{\partial y} &= 0, & \frac{\partial \vec{u}(x, L_y, z, t)}{\partial y} &= 0 \\ \frac{\partial \vec{u}(x, y, 0, t)}{\partial z} &= 0, & \frac{\partial \vec{u}(x, y, L_z, t)}{\partial z} &= 0 \\ \vec{u}(x, y, z, 0) &= \vec{u}_0 & \vec{u}(x, y, z, \infty) &= \vec{u}_0 \end{aligned} \quad (13)$$

We determined the spatio-temporal distributions of dopant concentration and radiation defects by solving Equations (1), (4), (7a) and (7b) using the standard method of averaging function corrections [28]. First, we transformed the Equations (1), (4), (7a) and (7b) into Equation (14), considering the initial distributions of the considered concentrations.

$$\begin{aligned} \frac{\partial C(x, y, z, t)}{\partial t} &= \frac{\partial}{\partial x} \left[ D \frac{\partial C(x, y, z, t)}{\partial x} \right] + \frac{\partial}{\partial y} \left[ D \frac{\partial C(x, y, z, t)}{\partial y} \right] + \frac{\partial}{\partial z} \left[ D \frac{\partial C(x, y, z, t)}{\partial z} \right] + \frac{\partial}{\partial \vec{x}} \left[ \frac{D_{CS}}{\bar{V}kT} \frac{\partial \mu_2(x, y, z, t)}{\partial x} \right] \\ &\quad + \frac{\partial}{\partial \vec{y}} \left[ \frac{D_{CS}}{\bar{V}kT} \frac{\partial \mu_2(x, y, z, t)}{\partial y} \right] + \frac{\partial}{\partial \vec{z}} \left[ \frac{D_{CS}}{\bar{V}kT} \frac{\partial \mu_2(x, y, z, t)}{\partial z} \right] \\ &\quad + \Omega \frac{\partial}{\partial x} \left[ \frac{D_S}{kT} \nabla_S \mu(x, y, z, t) \int_0^{L_x} C(x, y, W, t) dW \right] + \Omega \frac{\partial}{\partial y} \left[ \frac{D_S}{kT} \nabla_S \mu(x, y, z, t) \int_0^{L_y} C(x, y, W, t) dW \right] \end{aligned} \quad (14a)$$

$$\begin{aligned} \frac{\partial I(x, y, z, t)}{\partial t} &= \frac{\partial}{\partial x} \left[ D_I(x, y, z, T) \frac{\partial I(x, y, z, t)}{\partial x} \right] + \frac{\partial}{\partial y} \left[ D_I(x, y, z, T) \frac{\partial I(x, y, z, t)}{\partial y} \right] + \frac{\partial}{\partial z} \left[ D_I(x, y, z, T) \frac{\partial I(x, y, z, t)}{\partial z} \right] \\ &\quad + \Omega \frac{\partial}{\partial x} \left[ \frac{D_{IS}}{kT} \nabla_S \mu_1(x, y, z, t) \int_0^{L_x} I(x, y, W, t) dW \right] + \Omega \frac{\partial}{\partial y} \left[ \frac{D_{IS}}{kT} \nabla_S \mu_1(x, y, z, t) \int_0^{L_y} I(x, y, W, t) dW \right] \\ &\quad - k_{I,I}(x, y, z, T) I^2(x, y, z, t) - k_{I,V}(x, y, z, T) I(x, y, z, T) V(x, y, z, t) + f_I(x, y, z) \delta(t) \end{aligned} \quad (14b)$$

$$\begin{aligned} \frac{\partial V(x, y, z, t)}{\partial t} &= \frac{\partial}{\partial x} \left[ D_V(x, y, z, T) \frac{\partial V(x, y, z, t)}{\partial x} \right] + \frac{\partial}{\partial y} \left[ D_V(x, y, z, T) \frac{\partial V(x, y, z, t)}{\partial y} \right] + \Omega \frac{\partial}{\partial y} \left[ \frac{D_{IS}}{kT} \nabla_S \mu_1(x, y, z, t) \int_0^{L_y} I(x, y, W, t) dW \right] \\ &\quad - k_{V,I}(x, y, z, T) I^2(x, y, z, t) - k_{V,V}(x, y, z, T) I(x, y, z, T) V(x, y, z, t) + f_V(x, y, z) \delta(t) \end{aligned}$$

$$\begin{aligned} \frac{\partial \Phi_I(x, y, z, t)}{\partial t} &= \frac{\partial}{\partial x} \left[ D_{\Phi_I}(x, y, z, T) \frac{\partial \Phi_I(x, y, z, t)}{\partial x} \right] + \frac{\partial}{\partial y} \left[ D_{\Phi_I}(x, y, z, T) \frac{\partial \Phi_I(x, y, z, t)}{\partial y} \right] + \frac{\partial}{\partial z} \left[ D_{\Phi_I}(x, y, z, T) \frac{\partial \Phi_I(x, y, z, t)}{\partial z} \right] \\ &\quad + \Omega \frac{\partial}{\partial x} \left[ \frac{D_{\Phi_{IS}}}{kT} \nabla_S \mu_1(x, y, z, t) \int_0^{L_x} \Phi_I(x, y, W, t) dW \right] + \Omega \frac{\partial}{\partial y} \left[ \frac{D_{\Phi_{IS}}}{kT} \nabla_S \mu_1(x, y, z, t) \int_0^{L_y} \Phi_I(x, y, W, t) dW \right] \\ &\quad + k_I(x, y, z, T) I(x, y, z, t) + \frac{\partial}{\partial x} \left[ \frac{D_{\Phi_{IS}}}{\bar{V}kT} \frac{\partial \mu_2(x, y, z, t)}{\partial x} \right] + \frac{\partial}{\partial y} \left[ \frac{D_{\Phi_{IS}}}{\bar{V}kT} \frac{\partial \mu_2(x, y, z, t)}{\partial y} \right] + \frac{\partial}{\partial z} \left[ \frac{D_{\Phi_{IS}}}{\bar{V}kT} \frac{\partial \mu_2(x, y, z, t)}{\partial z} \right] \\ &\quad + k_{I,I}(x, y, z, T) I^2(x, y, z, t) + f_{\Phi_I}(x, y, z) \delta(t) \end{aligned} \quad (14c)$$

$$\begin{aligned} \frac{\partial \Phi_V(x, y, z, t)}{\partial t} &= \frac{\partial}{\partial x} \left[ D_{\Phi_V}(x, y, z, T) \frac{\partial \Phi_V(x, y, z, t)}{\partial x} \right] + \frac{\partial}{\partial y} \left[ D_{\Phi_V}(x, y, z, T) \frac{\partial \Phi_V(x, y, z, t)}{\partial y} \right] + \frac{\partial}{\partial z} \left[ D_{\Phi_V}(x, y, z, T) \frac{\partial \Phi_V(x, y, z, t)}{\partial z} \right] \\ &\quad + \Omega \frac{\partial}{\partial x} \left[ \frac{D_{\Phi_{VS}}}{kT} \nabla_S \mu_1(x, y, z, t) \int_0^{L_x} \Phi_V(x, y, W, t) dW \right] + \Omega \frac{\partial}{\partial y} \left[ \frac{D_{\Phi_{VS}}}{kT} \nabla_S \mu_1(x, y, z, t) \int_0^{L_y} \Phi_V(x, y, W, t) dW \right] \\ &\quad + k_V(x, y, z, T) I(x, y, z, t) + \frac{\partial}{\partial x} \left[ \frac{D_{\Phi_{VS}}}{\bar{V}kT} \frac{\partial \mu_2(x, y, z, t)}{\partial x} \right] + \frac{\partial}{\partial y} \left[ \frac{D_{\Phi_{VS}}}{\bar{V}kT} \frac{\partial \mu_2(x, y, z, t)}{\partial y} \right] + \frac{\partial}{\partial z} \left[ \frac{D_{\Phi_{VS}}}{\bar{V}kT} \frac{\partial \mu_2(x, y, z, t)}{\partial z} \right] \\ &\quad + k_{V,V}(x, y, z, T) V^2(x, y, z, t) + f_{\Phi_V}(x, y, z) \delta(t) \end{aligned}$$

Next, we replaced the concentrations of dopant and radiation defects on the right-hand sides of Equations (14a), (14b) and (14c) with their unknown average values, denoted by  $\alpha_{1\rho}$ . This allowed us to obtain equations for the first-order

$$\begin{aligned} \frac{\partial C_1(x, y, z, t)}{\partial t} &= \alpha_{1C} \Omega \frac{\partial}{\partial x} \left[ z \frac{D_S}{kT} \nabla_S \mu_1(x, y, z, t) \right] + \alpha_{1C} \Omega \frac{\partial}{\partial y} \left[ z \frac{D_S}{kT} \nabla_S \mu_1(x, y, z, t) \right] + \frac{\partial \mu_2(x, y, z, t)}{\partial x} d\tau + \frac{\partial}{\partial \vec{y}} \int_0^t \frac{D_{CS}}{\bar{V}kT} \frac{\partial \mu_2(x, y, z, \tau)}{\partial y} d\tau \\ &\quad + \frac{\partial}{\partial \vec{z}} \int_0^t \frac{D_{CS}}{\bar{V}kT} \frac{\partial \mu_2(x, y, z, \tau)}{\partial z} d\tau + f_C(x, y, z) \delta(t) \end{aligned} \quad (15a)$$

$$\begin{aligned} \frac{\partial I_1(x, y, z, t)}{\partial t} &= \alpha_{1I} z \Omega \frac{\partial}{\partial x} \left[ \frac{D_{IS}}{kT} \nabla_S \mu_1(x, y, z, t) \right] + \alpha_{1I} \Omega \frac{\partial}{\partial y} \left[ z \frac{D_{IS}}{kT} \nabla_S \mu_1(x, y, z, t) \right] + \frac{\partial}{\partial x} \left[ \frac{D_{IS}}{\bar{V}kT} \frac{\partial \mu_2(x, y, z, t)}{\partial x} \right] + \frac{\partial}{\partial y} \left[ \frac{D_{IS}}{\bar{V}kT} \frac{\partial \mu_2(x, y, z, t)}{\partial y} \right] \\ &\quad + \frac{\partial}{\partial z} \left[ \frac{D_{IS}}{\bar{V}kT} \frac{\partial \mu_2(x, y, z, t)}{\partial z} \right] + f_I(x, y, z) \delta(t) - \alpha_{1I}^2 k_{I,I}(x, y, z, T) - \alpha_{1I} \alpha_{1V} k_{I,V}(x, y, z, T) \end{aligned} \quad (15b)$$

$$\begin{aligned} \frac{\partial V_1(x, y, z, t)}{\partial t} &= \alpha_{1V} z \Omega \frac{\partial}{\partial x} \left[ \frac{D_{VS}}{kT} \nabla_S \mu_1(x, y, z, t) \right] + \alpha_{1V} \Omega \frac{\partial}{\partial y} \left[ z \frac{D_{VS}}{kT} \nabla_S \mu_1(x, y, z, t) \right] + \frac{\partial}{\partial x} \left[ \frac{D_{VS}}{\bar{V}kT} \frac{\partial \mu_2(x, y, z, t)}{\partial x} \right] + \frac{\partial}{\partial y} \left[ \frac{D_{VS}}{\bar{V}kT} \frac{\partial \mu_2(x, y, z, t)}{\partial y} \right] \\ &\quad + \frac{\partial}{\partial z} \left[ \frac{D_{VS}}{\bar{V}kT} \frac{\partial \mu_2(x, y, z, t)}{\partial z} \right] + f_V(x, y, z) \delta(t) - \alpha_{1V}^2 k_{V,V}(x, y, z, T) - \alpha_{1I} \alpha_{1V} k_{I,V}(x, y, z, T) \end{aligned} \quad (15c)$$

approximations of the required concentrations, as shown in Equations (15a), (15b) and (15c).

$$\begin{aligned} \frac{\partial \Phi_{1I}(x, y, z, t)}{\partial t} &= \alpha_{1\Phi_I} z \Omega \frac{\partial}{\partial x} \left[ \frac{D_{\Phi_{IS}}}{kT} \nabla_S \mu_1(x, y, z, t) \right] + \alpha_{1\Phi_I} z \Omega \frac{\partial}{\partial y} \left[ \frac{D_{\Phi_{IS}}}{kT} \nabla_S \mu_1(x, y, z, t) \right] + \frac{\partial}{\partial x} \left[ \frac{D_{\Phi_{IS}} \partial \mu_2(x, y, z, t)}{\bar{V}kT} \right] + \frac{\partial}{\partial y} \left[ \frac{D_{\Phi_{IS}} \partial \mu_2(x, y, z, t)}{\bar{V}kT} \right] \\ &\quad + \frac{\partial}{\partial z} \left[ \frac{D_{\Phi_{IS}} \partial \mu_2(x, y, z, t)}{\bar{V}kT} \right] + f_{\Phi_I}(x, y, z) \delta(t) + k_I(x, y, z, T) I(x, y, z, t) + k_{I,I}(x, y, z, T) I^2(x, y, z, t) \end{aligned}$$

$$\begin{aligned} \frac{\partial \Phi_{1V}(x, y, z, t)}{\partial t} &= \alpha_{1\Phi_V} z \Omega \frac{\partial}{\partial x} \left[ \frac{D_{\Phi_{VS}}}{kT} \nabla_S \mu_1(x, y, z, t) \right] + \alpha_{1\Phi_V} z \Omega \frac{\partial}{\partial y} \left[ \frac{D_{\Phi_{VS}}}{kT} \nabla_S \mu_1(x, y, z, t) \right] + \frac{\partial}{\partial x} \left[ \frac{D_{\Phi_{VS}} \partial \mu_2(x, y, z, t)}{\bar{V}kT} \right] \\ &\quad + \frac{\partial}{\partial y} \left[ \frac{D_{\Phi_{VS}} \partial \mu_2(x, y, z, t)}{\bar{V}kT} \right] + \frac{\partial}{\partial z} \left[ \frac{D_{\Phi_{VS}} \partial \mu_2(x, y, z, t)}{\bar{V}kT} \right] + f_{\Phi_V}(x, y, z) \delta(t) + k_V(x, y, z, T) V(x, y, z, t) \\ &\quad + k_{V,V}(x, y, z, T) V^2(x, y, z, t) \end{aligned}$$

Integrating both sides of Equations (15a), (15b) and (15c) over time enabled us to derive the relations for above approximations in their final form, as given in Equations (16a), (16b) and (16c).

$$\begin{aligned} C_1(x, y, z, t) &= \alpha_{1C} \Omega \frac{\partial}{\partial x} \int_0^t D_{SL}(x, y, z, T) \frac{z}{kT} \left[ 1 + \zeta_1 \frac{V(x, y, z, \tau)}{V^*} + \zeta_2 \frac{V^2(x, y, z, \tau)}{(V^*)^2} \right] \times \\ &\quad \times \Omega \nabla_S \mu_1(x, y, z, \tau) \frac{z}{kT} \left[ 1 + \zeta_1 \frac{V(x, y, z, \tau)}{V^*} + \zeta_2 \frac{V^2(x, y, z, \tau)}{(V^*)^2} \right] d\tau + f_C(x, y, z) + \frac{\partial}{\partial \vec{x}} \int_0^t \frac{D_{CS}}{\bar{V}kT} \times \frac{\partial \mu_2(x, y, z, \tau)}{\partial x} d\tau \\ &\quad + \frac{\partial}{\partial \vec{y}} \int_0^t \frac{D_{CS}}{\bar{V}kT} \frac{\partial \mu_2(x, y, z, \tau)}{\partial y} d\tau + \frac{\partial}{\partial \vec{z}} \int_0^t \frac{D_{CS}}{\bar{V}kT} \frac{\partial \mu_2(x, y, z, \tau)}{\partial z} d\tau \end{aligned} \quad (16a)$$

$$\begin{aligned} I_1(x, y, z, t) &= \alpha_{1I} z \Omega \frac{\partial}{\partial x} \int_0^t \frac{D_{IS}}{kT} \nabla_S \mu_1(x, y, z, \tau) d\tau + \alpha_{1I} z \Omega \frac{\partial}{\partial y} \int_0^t \frac{D_{IS}}{kT} \nabla_S \mu_1(x, y, z, \tau) d\tau + \frac{\partial}{\partial x} \int_0^t \frac{D_{IS}}{\bar{V}kT} \frac{\partial \mu_2(x, y, z, \tau)}{\partial x} d\tau \\ &\quad + \frac{\partial}{\partial y} \int_0^t \frac{D_{IS}}{\bar{V}kT} \frac{\partial \mu_2(x, y, z, \tau)}{\partial y} d\tau + \frac{\partial}{\partial z} \int_0^t \frac{D_{IS}}{\bar{V}kT} \frac{\partial \mu_2(x, y, z, \tau)}{\partial z} d\tau + f_I(x, y, z) - \alpha_{1I}^2 \int_0^t k_{I,I}(x, y, z, T) d\tau \\ &\quad - \alpha_{1I} \alpha_{1V} \int_0^t k_{I,V}(x, y, z, T) d\tau \end{aligned} \quad (16b)$$

$$\begin{aligned} V_1(x, y, z, t) &= \alpha_{1V} z \Omega \frac{\partial}{\partial x} \int_0^t \frac{D_{IS}}{kT} \nabla_S \mu_1(x, y, z, \tau) d\tau + \alpha_{1V} z \Omega \frac{\partial}{\partial y} \int_0^t \frac{D_{IS}}{kT} \nabla_S \mu_1(x, y, z, \tau) d\tau + \frac{\partial}{\partial x} \int_0^t \frac{D_{VS}}{\bar{V}kT} \frac{\partial \mu_2(x, y, z, \tau)}{\partial x} d\tau \\ &\quad + \frac{\partial}{\partial y} \int_0^t \frac{D_{VS}}{\bar{V}kT} \frac{\partial \mu_2(x, y, z, \tau)}{\partial y} d\tau + \frac{\partial}{\partial z} \int_0^t \frac{D_{VS}}{\bar{V}kT} \frac{\partial \mu_2(x, y, z, \tau)}{\partial z} d\tau + f_V(x, y, z) - \alpha_{1V}^2 \int_0^t k_{V,V}(x, y, z, T) d\tau \\ &\quad - \alpha_{1I} \alpha_{1V} \int_0^t k_{I,V}(x, y, z, T) d\tau \end{aligned}$$

$$\begin{aligned} \Phi_{1I}(x, y, z, t) &= \alpha_{1\Phi_I} z \Omega \frac{\partial}{\partial x} \int_0^t \frac{D_{\Phi_{IS}}}{kT} \nabla_S \mu_1(x, y, z, \tau) d\tau + \alpha_{1\Phi_I} z \Omega \frac{\partial}{\partial y} \int_0^t \frac{D_{\Phi_{IS}}}{kT} \nabla_S \mu_1(x, y, z, \tau) d\tau \times \alpha_{1\Phi_I} z + f_{\Phi_I}(x, y, z) + \frac{\partial}{\partial x} \int_0^t \frac{D_{\Phi_{IS}}}{\bar{V}kT} \frac{\partial \mu_2(x, y, z, \tau)}{\partial x} d\tau \\ &\quad + \frac{\partial}{\partial y} \int_0^t \frac{D_{\Phi_{IS}}}{\bar{V}kT} \frac{\partial \mu_2(x, y, z, \tau)}{\partial y} d\tau + \frac{\partial}{\partial z} \int_0^t \frac{D_{\Phi_{IS}}}{\bar{V}kT} \frac{\partial \mu_2(x, y, z, \tau)}{\partial z} d\tau + \int_0^t k_I(x, y, z, T) I(x, y, z, \tau) d\tau \\ &\quad + \int_0^t k_{I,I}(x, y, z, T) I^2(x, y, z, \tau) d\tau \end{aligned} \quad (16c)$$

$$\begin{aligned} \Phi_{1V}(x, y, z, t) &= \alpha_{1\Phi_V} z \Omega \frac{\partial}{\partial x} \int_0^t \frac{D_{\Phi_{VS}}}{kT} \nabla_S \mu_1(x, y, z, \tau) d\tau + \alpha_{1\Phi_V} z \Omega \frac{\partial}{\partial y} \int_0^t \frac{D_{\Phi_{VS}}}{kT} \nabla_S \mu_1(x, y, z, \tau) d\tau \times \alpha_{1\Phi_V} z + f_{\Phi_V}(x, y, z) \\ &\quad + \frac{\partial}{\partial x} \int_0^t \frac{D_{\Phi_{VS}}}{\bar{V}kT} \frac{\partial \mu_2(x, y, z, \tau)}{\partial x} d\tau + \frac{\partial}{\partial y} \int_0^t \frac{D_{\Phi_{VS}}}{\bar{V}kT} \frac{\partial \mu_2(x, y, z, \tau)}{\partial y} d\tau + \frac{\partial}{\partial z} \int_0^t \frac{D_{\Phi_{VS}}}{\bar{V}kT} \frac{\partial \mu_2(x, y, z, \tau)}{\partial z} d\tau \\ &\quad + \int_0^t k_V(x, y, z, T) V(x, y, z, \tau) d\tau + \int_0^t k_{V,V}(x, y, z, T) V^2(x, y, z, \tau) d\tau \end{aligned}$$

We determined the average values of the first-order approximations of the concentrations of dopant and radiation defects by following the standard relation, as shown in Equation (17) [28]

$$\alpha_{1\rho} = \frac{1}{\theta L_x L_y L_z} \int_0^\theta \int_0^{L_x} \int_0^{L_y} \int_0^{L_z} \rho_1(x, y, z, t) dz dy dx dt \quad (17)$$

Substituting the relations from Equations (16a), (16b) and (16c) into Equation (17) allowed us to obtain the required average values, as shown in Equation (18a).

$$\begin{aligned} \alpha_{1C} &= \frac{1}{L_x L_y L_z} \int_0^{L_x} \int_0^{L_y} \int_0^{L_z} f_C(x, y, z) dz dy dx \\ \alpha_{1I} &= \sqrt{\frac{(a_3 + A)^2}{4a_4^2} - 4 \left( B + \frac{\theta a_3 B + \theta^2 L_x L_y L_z a_1}{a_4} \right)} - \frac{a_3 + A}{4a_4} \\ \alpha_{1V} &= \frac{1}{S_{IV00}} \left[ \frac{\theta}{\alpha_{1I}} \int_0^{L_x} \int_0^{L_y} \int_0^{L_z} f_I(x, y, z) dz dy dx - \alpha_{1I} S_{II00} - \theta L_x L_y L_z \right] \end{aligned} \quad (18a)$$

where

$$\begin{aligned} S_{\rho\rho ij} &= \int_0^\theta (\theta - t) \int_0^{L_x} \int_0^{L_y} \int_0^{L_z} k_{\rho,\rho}(x, y, z, T) I_1^i(x, y, z, t) V_1^j(x, y, z, t) dz dy dx dt \\ a_4 &= S_{II00} \times (S_{IV00}^2 - S_{II00} S_{VV00}) \\ a_3 &= S_{IV00} S_{II00} + S_{IV00}^2 - S_{II00} S_{VV00} \end{aligned} \quad (18b)$$

$$\begin{aligned}
 a_2 &= \int_0^{L_x} \int_0^{L_y} \int_0^{L_z} f_v(x, y, z) dz dy dx \times S_{IV00} S_{IV00}^2 + S_{IV00} \theta L_x^2 L_y^2 L_z^2 + 2 S_{VV00} S_{II00} \int_0^{L_x} \int_0^{L_y} \int_0^{L_z} f_l(x, y, z) dz dy dx - \theta L_x^2 L_y^2 L_z^2 S_{VV00} \\
 &\quad - S_{IV00}^2 \int_0^{L_x} \int_0^{L_y} \int_0^{L_z} f_l(x, y, z) dz dy dx \\
 a_1 &= S_{IV00} \int_0^{L_x} \int_0^{L_y} \int_0^{L_z} f_l(x, y, z) dz dy dx \\
 a_0 &= S_{VV00} \times \left[ \int_0^{L_x} \int_0^{L_y} \int_0^{L_z} f_l(x, y, z) dz dy dx \right]^2 \\
 A &= \sqrt{\frac{8y + \theta^2 \frac{a_3^2}{a_4^2} - 4\theta \frac{a_2}{a_4}}{8a_4^2}} \\
 B &= \frac{\theta a_2}{6a_4} + \sqrt[3]{\sqrt{q^2 + p^3} - q} - \sqrt[3]{\sqrt{q^2 + p^3} + q} \\
 q &= \frac{\theta^3 a_2}{24a_4^2} \left( 4a_0 - \theta L_x L_y L_z \frac{a_1 a_3}{a_4} \right) - \theta^2 \frac{a_0}{8a_4^2} \left( 4\theta a_2 - \theta^2 \frac{a_3^2}{a_4^2} \right) - \frac{\theta^3 a_2^3}{54a_4^3} - L_x^2 L_y^2 L_z^2 \frac{\theta^4 a_1^2}{8a_4^2} \\
 p &= \theta^2 \frac{4a_0 a_4 - \theta L_x L_y L_z a_1 a_3}{12a_4^2} - \frac{\theta a_2}{18a_4} \\
 a_{1\phi_l} &= \frac{R_{I1}}{\theta L_x L_y L_z} + \frac{S_{II20}}{\theta L_x L_y L_z} + \frac{1}{L_x L_y L_z} \int_0^{L_x} \int_0^{L_y} \int_0^{L_z} f_{\phi_l}(x, y, z) dz dy dx \\
 a_{1\phi_v} &= \frac{R_{V1}}{\theta L_x L_y L_z} + \frac{S_{VV20}}{\theta L_x L_y L_z} + \frac{1}{L_x L_y L_z} \int_0^{L_x} \int_0^{L_y} \int_0^{L_z} f_{\phi_v}(x, y, z) dz dy dx
 \end{aligned}$$

where

$$\begin{aligned}
 R_{\rho_l} \\
 = \int_0^\theta (\theta \\
 - t) \int_0^{L_x} \int_0^{L_y} \int_0^{L_z} k_l(x, y, z, T) I_l^i(x, y, z, t) dz dy dx dt
 \end{aligned} \tag{18c}$$

We determined the second and higher orders approximation of the concentrations of dopant and radiation defects using the standard iterative procedure of the method of averaging

$$\begin{aligned}
 \frac{\partial C_2(x, y, z, t)}{\partial t} &= \frac{\partial}{\partial x} \left( \left\{ 1 + \xi \frac{[\alpha_{2C} + C_1(x, y, z, t)]^y}{PV(x, y, z, T)} \right\} \left[ 1 + \varsigma_1 \frac{V(x, y, z, t)}{V^*} + \varsigma_2 \frac{V^2(x, y, z, t)}{(V^*)^2} \right] \times D_L(x, y, z, T) \frac{\partial C_1(x, y, z, t)}{\partial x} \right) \\
 &\quad + \frac{\partial}{\partial y} \left( \left\{ 1 + \varsigma_1 \frac{V(x, y, z, t)}{V^*} + \varsigma_2 \frac{V^2(x, y, z, t)}{(V^*)^2} \right\} \frac{\partial C_1(x, y, z, t)}{\partial y} \times D_L(x, y, z, T) \left\{ 1 + \xi \frac{[\alpha_{2C} + C_1(x, y, z, t)]^y}{PV(x, y, z, T)} \right\} \right) \\
 &\quad + \frac{\partial}{\partial z} \left( \left\{ 1 + \varsigma_1 \frac{V(x, y, z, t)}{V^*} + \varsigma_2 \frac{V^2(x, y, z, t)}{(V^*)^2} \right\} \times D_L(x, y, z, T) \frac{\partial C_1(x, y, z, t)}{\partial z} \left\{ 1 + \xi \frac{[\alpha_{2C} + C_1(x, y, z, t)]^y}{PV(x, y, z, T)} \right\} \right) \\
 &\quad + f_C(x, y, z) \delta(t) + \frac{\partial}{\partial \vec{x}} \left[ \frac{D_{CS}}{VKT} \frac{\partial \mu_2(x, y, z, t)}{\partial x} \right] + \frac{\partial}{\partial \vec{y}} \left[ \frac{D_{CS}}{VKT} \frac{\partial \mu_2(x, y, z, t)}{\partial y} \right] + \frac{\partial}{\partial \vec{z}} \left[ \frac{D_{CS}}{VKT} \frac{\partial \mu_2(x, y, z, t)}{\partial z} \right]
 \end{aligned} \tag{19a}$$

$$\begin{aligned}
 \frac{\partial I_2(x, y, z, t)}{\partial t} &= \frac{\partial}{\partial x} \left[ D_l(x, y, z, T) \frac{\partial I_l(x, y, z, t)}{\partial x} \right] + \frac{\partial}{\partial y} \left[ D_l(x, y, z, T) \frac{\partial I_l(x, y, z, t)}{\partial y} \right] + \frac{\partial}{\partial z} \left[ D_l(x, y, z, T) \frac{\partial I_l(x, y, z, t)}{\partial z} \right] \\
 &\quad - k_{l,l}(x, y, z, T) [\alpha_{1l} + I_1(x, y, z, t)]^2 - k_{l,v}(x, y, z, T) \times [\alpha_{1l} + I_1(x, y, z, t)] [\alpha_{1v} + V_1(x, y, z, t)] \\
 &\quad + \Omega \frac{\partial}{\partial x} \left\{ \nabla_S \mu(x, y, z, t) \int_0^{L_z} [\alpha_{2l} + I_1(x, y, W, t)] dW \times \frac{D_{IS}}{kT} \right\} + \Omega \frac{\partial}{\partial y} \left\{ \frac{D_{IS}}{kT} \nabla_S \mu(x, y, z, t) \int_0^{L_z} [\alpha_{2l} + I_1(x, y, W, t)] dW \right\} \\
 &\quad + \frac{\partial}{\partial x} \int_0^t \frac{\partial \mu_2(x, y, z, t)}{\partial x} \times \frac{D_{IS}}{VKT} dt + \frac{\partial}{\partial y} \int_0^t \frac{D_{IS}}{VKT} \frac{\partial \mu_2(x, y, z, t)}{\partial y} dt + \frac{\partial}{\partial z} \int_0^t \frac{D_{IS}}{VKT} \frac{\partial \mu_2(x, y, z, t)}{\partial z} dt
 \end{aligned} \tag{19b}$$

$$\begin{aligned}
 \frac{\partial V_2(x, y, z, t)}{\partial t} &= \frac{\partial}{\partial x} \left[ D_V(x, y, z, T) \frac{\partial V_1(x, y, z, t)}{\partial x} \right] + \frac{\partial}{\partial y} \left[ D_V(x, y, z, T) \frac{\partial V_1(x, y, z, t)}{\partial y} \right] + \frac{\partial}{\partial z} \left[ D_V(x, y, z, T) \frac{\partial V_1(x, y, z, t)}{\partial z} \right] \\
 &\quad - k_{V,V}(x, y, z, T) [\alpha_{1V} + V_1(x, y, z, t)]^2 - k_{l,V}(x, y, z, T) \times [\alpha_{1l} + I_1(x, y, z, t)] [\alpha_{1V} + V_1(x, y, z, t)] \\
 &\quad + \Omega \frac{\partial}{\partial x} \left\{ \nabla_S \mu(x, y, z, t) \int_0^{L_z} [\alpha_{2V} + V_1(x, y, W, t)] dW \times \frac{D_{VS}}{kT} \right\} \\
 &\quad + \Omega \frac{\partial}{\partial y} \left\{ \frac{D_{VS}}{kT} \nabla_S \mu(x, y, z, t) \int_0^{L_z} [\alpha_{2V} + V_1(x, y, W, t)] dW \right\} + \frac{\partial}{\partial x} \int_0^t \frac{\partial \mu_2(x, y, z, t)}{\partial x} \times \frac{D_{VS}}{VKT} dt \\
 &\quad + \frac{\partial}{\partial y} \int_0^t \frac{D_{VS}}{VKT} \frac{\partial \mu_2(x, y, z, t)}{\partial y} dt + \frac{\partial}{\partial z} \int_0^t \frac{D_{VS}}{VKT} \frac{\partial \mu_2(x, y, z, t)}{\partial z} dt
 \end{aligned} \tag{19c}$$

$$\begin{aligned}
 \frac{\partial \Phi_{2l}(x, y, z, t)}{\partial t} &= \frac{\partial}{\partial x} \left[ D_{\phi_l}(x, y, z, T) \frac{\partial \Phi_{1l}(x, y, z, t)}{\partial x} \right] + \frac{\partial}{\partial y} \left[ D_{\phi_l}(x, y, z, T) \frac{\partial \Phi_{1l}(x, y, z, t)}{\partial y} \right] \\
 &\quad + \Omega \frac{\partial}{\partial x} \left\{ \frac{D_{\phi_{1S}}}{kT} \nabla_S \mu(x, y, z, t) \int_0^{L_z} [\alpha_{2\phi_l} + \Phi_{1l}(x, y, W, t)] dW \right\} + k_{l,l}(x, y, z, T) I^2(x, y, z, t) \\
 &\quad + \Omega \frac{\partial}{\partial y} \left\{ \frac{D_{\phi_{1S}}}{kT} \nabla_S \mu(x, y, z, t) \int_0^{L_z} [\alpha_{2\phi_l} + \Phi_{1l}(x, y, W, t)] dW \right\} + k_l(x, y, z, T) I(x, y, z, t) + \frac{\partial}{\partial x} \left[ \frac{D_{\phi_{1S}}}{VKT} \frac{\partial \mu_2(x, y, z, t)}{\partial x} \right] \\
 &\quad + \frac{\partial}{\partial y} \left[ \frac{D_{\phi_{1S}}}{VKT} \frac{\partial \mu_2(x, y, z, t)}{\partial y} \right] + \frac{\partial}{\partial z} \left[ \frac{D_{\phi_{1S}}}{VKT} \frac{\partial \mu_2(x, y, z, t)}{\partial z} \right] + \frac{\partial}{\partial z} \left[ D_{\phi_l}(x, y, z, T) \frac{\partial \Phi_{1l}(x, y, z, t)}{\partial z} \right] + f_{\phi_l}(x, y, z) \delta(t)
 \end{aligned}$$

function corrections [28]. Within this procedure, to determine the  $n$ -th order approximations of the concentrations, we replaced the required concentrations in Equations (16a), (16b), (16c) with the sum  $\alpha_{n\rho} + \rho_{n-1}(x, y, z, t)$ . This replacement leads to the transformation of the corresponding equations, as shown in Equations (19a), (19b) and (19c).

$$\begin{aligned} \frac{\partial \Phi_{2V}(x, y, z, t)}{\partial t} = & \frac{\partial}{\partial x} \left[ D_{\Phi_V}(x, y, z, T) \frac{\partial \Phi_{1V}(x, y, z, t)}{\partial x} \right] + \frac{\partial}{\partial y} \left[ D_{\Phi_V}(x, y, z, T) \frac{\partial \Phi_{1V}(x, y, z, t)}{\partial y} \right] \\ & + \Omega \frac{\partial}{\partial x} \left( \frac{D_{\Phi_V S}}{kT} \nabla_S \mu(x, y, z, t) \int_0^{Lz} [\alpha_{2\Phi_V} + \Phi_{1V}(x, y, W, t)] dW \right) + k_{V,V}(x, y, z, T) V^2(x, y, z, t) \\ & + \Omega \frac{\partial}{\partial y} \left( \frac{D_{\Phi_V S}}{kT} \nabla_S \mu(x, y, z, t) \int_0^{Lz} [\alpha_{2\Phi_V} + \Phi_{1V}(x, y, W, t)] dW \right) + k_V(x, y, z, T) V(x, y, z, t) \\ & + \frac{\partial}{\partial x} \left[ \frac{D_{\Phi_V S} \partial \mu_2(x, y, z, t)}{\bar{V}kT} \right] + \frac{\partial}{\partial y} \left[ \frac{D_{\Phi_V S} \partial \mu_2(x, y, z, t)}{\bar{V}kT} \right] + \frac{\partial}{\partial z} \left[ \frac{D_{\Phi_V S} \partial \mu_2(x, y, z, t)}{\bar{V}kT} \right] \\ & + \frac{\partial}{\partial z} \left[ D_{\Phi_V}(x, y, z, T) \frac{\partial \Phi_{1V}(x, y, z, t)}{\partial z} \right] + f_{\Phi_V}(x, y, z) \delta(t) \end{aligned}$$

Integrating both sides of Equations (19a), (19b) and (19c) allows us to obtain the relations for the required concentrations in their final form, as shown in Equations (20a), (20b) and (20c).

$$\begin{aligned} C_2(x, y, z, t) = & \frac{\partial}{\partial x} \int_0^t \left\{ 1 + \xi \frac{[\alpha_{2C} + C_1(x, y, z, \tau)]^y}{P^y(x, y, z, T)} \right\} \left[ 1 + \varsigma_1 \frac{V(x, y, z, \tau)}{V^*} + \varsigma_2 \frac{V^2(x, y, z, \tau)}{(V^*)^2} \right] \times D_L(x, y, z, T) \frac{\partial C_1(x, y, z, \tau)}{\partial x} d\tau \\ & + \frac{\partial}{\partial y} \int_0^t D_L(x, y, z, T) \left[ 1 + \varsigma_1 \frac{V(x, y, z, \tau)}{V^*} + \varsigma_2 \frac{V^2(x, y, z, \tau)}{(V^*)^2} \right] \times \frac{\partial C_1(x, y, z, \tau)}{\partial y} \left\{ 1 + \xi \frac{[\alpha_{2C} + C_1(x, y, z, \tau)]^y}{P^y(x, y, z, T)} \right\} \\ & + \frac{\partial}{\partial z} \int_0^t \left[ 1 + \varsigma_1 \frac{V(x, y, z, \tau)}{V^*} + \varsigma_2 \frac{V^2(x, y, z, \tau)}{(V^*)^2} \right] \times D_L(x, y, z, T) \frac{\partial C_1(x, y, z, \tau)}{\partial z} \left\{ 1 + \xi \frac{[\alpha_{2C} + C_1(x, y, z, \tau)]^y}{P^y(x, y, z, T)} \right\} d\tau \\ & + f_C(x, y, z) + \Omega \frac{\partial}{\partial x} \int_0^t \frac{D_S}{kT} \nabla_S \mu(x, y, z, \tau) \int_0^{Lz} [\alpha_{2C} + C_1(x, y, W, \tau)] dW d\tau \\ & + \frac{\partial}{\partial y} \int_0^t \nabla_S \mu(x, y, z, \tau) \times \Omega \frac{D_S}{kT} \int_0^{Lz} [\alpha_{2C} + C_1(x, y, W, \tau)] dW d\tau + \frac{\partial}{\partial \vec{x} \cdot x} \left[ \frac{D_{CS}}{\bar{V}kT} \frac{\partial \mu_2(x, y, z, t)}{\partial x} \right] \\ & + \frac{\partial}{\partial \vec{x} \cdot y} \left[ \frac{D_{CS}}{\bar{V}kT} \frac{\partial \mu_2(x, y, z, t)}{\partial y} \right] + \frac{\partial}{\partial \vec{x} \cdot z} \left[ \frac{D_{CS}}{\bar{V}kT} \frac{\partial \mu_2(x, y, z, t)}{\partial z} \right] \end{aligned} \quad (20a)$$

$$\begin{aligned} I_2(x, y, z, t) = & \frac{\partial}{\partial x} \int_0^t D_I(x, y, z, T) \frac{\partial I_1(x, y, z, \tau)}{\partial x} d\tau + \frac{\partial}{\partial y} \int_0^t D_I(x, y, z, T) \frac{\partial I_1(x, y, z, \tau)}{\partial y} d\tau + \frac{\partial}{\partial z} \int_0^t D_I(x, y, z, T) \frac{\partial I_1(x, y, z, \tau)}{\partial z} d\tau \\ & - \int_0^t k_{I,I}(x, y, z, T) [\alpha_{2I} + I_1(x, y, z, \tau)]^2 d\tau - \int_0^t k_{I,V}(x, y, z, T) [\alpha_{2I} + I_1(x, y, z, \tau)] [\alpha_{2V} + V_1(x, y, z, \tau)] d\tau \\ & + \frac{\partial}{\partial x} \int_0^t \nabla_S \mu(x, y, z, \tau) \times \Omega \frac{D_{IS}}{kT} \int_0^{Lz} [\alpha_{2I} + I_1(x, y, W, \tau)] dW d\tau \\ & + \frac{\partial}{\partial y} \int_0^t \nabla_S \mu(x, y, z, \tau) \int_0^{Lz} [\alpha_{2I} + I_1(x, y, W, \tau)] \times \Omega \frac{D_{IS}}{kT} dW d\tau + \frac{\partial}{\partial \vec{x} \cdot x} \left[ \frac{D_{IS}}{\bar{V}kT} \frac{\partial \mu_2(x, y, z, t)}{\partial x} \right] \\ & + \frac{\partial}{\partial \vec{x} \cdot y} \left[ \frac{D_{IS}}{\bar{V}kT} \frac{\partial \mu_2(x, y, z, t)}{\partial y} \right] + \frac{\partial}{\partial \vec{x} \cdot z} \left[ \frac{D_{IS}}{\bar{V}kT} \frac{\partial \mu_2(x, y, z, t)}{\partial z} \right] + f_I(x, y, z) \end{aligned} \quad (20b)$$

$$\begin{aligned} V_2(x, y, z, t) = & \frac{\partial}{\partial x} \int_0^t D_V(x, y, z, T) \frac{\partial V_1(x, y, z, \tau)}{\partial x} d\tau + \frac{\partial}{\partial y} \int_0^t D_V(x, y, z, T) \frac{\partial V_1(x, y, z, \tau)}{\partial y} d\tau + \frac{\partial}{\partial z} \int_0^t D_V(x, y, z, T) \frac{\partial V_1(x, y, z, \tau)}{\partial z} d\tau \\ & - \int_0^t k_{V,V}(x, y, z, T) [\alpha_{2V} + V_1(x, y, z, \tau)]^2 d\tau - \int_0^t k_{I,V}(x, y, z, T) [\alpha_{2I} + I_1(x, y, z, \tau)] [\alpha_{2V} + V_1(x, y, z, \tau)] d\tau \\ & + \frac{\partial}{\partial x} \int_0^t \nabla_S \mu(x, y, z, \tau) \times \Omega \frac{D_{VS}}{kT} \int_0^{Lz} [\alpha_{2V} + V_1(x, y, W, \tau)] dW d\tau \\ & + \frac{\partial}{\partial y} \int_0^t \nabla_S \mu(x, y, z, \tau) \int_0^{Lz} [\alpha_{2V} + V_1(x, y, W, \tau)] \times \Omega \frac{D_{VS}}{kT} dW d\tau + \frac{\partial}{\partial \vec{x} \cdot x} \left[ \frac{D_{VS}}{\bar{V}kT} \frac{\partial \mu_2(x, y, z, t)}{\partial x} \right] \\ & + \frac{\partial}{\partial \vec{x} \cdot y} \left[ \frac{D_{VS}}{\bar{V}kT} \frac{\partial \mu_2(x, y, z, t)}{\partial y} \right] + \frac{\partial}{\partial \vec{x} \cdot z} \left[ \frac{D_{VS}}{\bar{V}kT} \frac{\partial \mu_2(x, y, z, t)}{\partial z} \right] + f_V(x, y, z) \end{aligned} \quad (20c)$$

$$\begin{aligned}\phi_{2l}(x, y, z, t) = & \frac{\partial}{\partial x} \int_0^t D_{\phi_l}(x, y, z, T) \frac{\partial \Phi_{1l}(x, y, z, \tau)}{\partial x} d\tau + \frac{\partial}{\partial y} \int_0^t \frac{\partial \Phi_{1l}(x, y, z, \tau)}{\partial y} \times D_{\phi_l}(x, y, z, T) d\tau \\ & + \frac{\partial}{\partial z} \int_0^t D_{\phi_l}(x, y, z, T) \frac{\partial \Phi_{1l}(x, y, z, \tau)}{\partial z} d\tau + \Omega \frac{\partial}{\partial x} \int_0^t \nabla_S \mu(x, y, z, \tau) \times \frac{D_{\phi_l S}}{kT} \int_0^{L_z} [\alpha_{2\phi_l} + \Phi_{1l}(x, y, W, \tau)] dW d\tau \\ & + \Omega \frac{\partial}{\partial y} \int_0^t \frac{D_{\phi_l S}}{kT} \int_0^{L_z} [\alpha_{2\phi_l} + \Phi_{1l}(x, y, W, \tau)] dW \times \nabla_S \mu(x, y, z, \tau) d\tau + \int_0^t k_{l,l}(x, y, z, T) I^2(x, y, z, \tau) d\tau \\ & + \frac{\partial}{\partial x} \int_0^t \frac{D_{\phi_l S}}{\bar{V}kT} \frac{\partial \mu_2(x, y, z, \tau)}{\partial x} d\tau + \frac{\partial}{\partial y} \int_0^t \frac{D_{\phi_l S}}{\bar{V}kT} \frac{\partial \mu_2(x, y, z, \tau)}{\partial y} d\tau + \frac{\partial}{\partial z} \int_0^t \frac{D_{\phi_l S}}{\bar{V}kT} \frac{\partial \mu_2(x, y, z, \tau)}{\partial z} d\tau + f_{\phi_l}(x, y, z) \\ & + \int_0^t k_l(x, y, z, T) I(x, y, z, \tau) d\tau\end{aligned}$$

The average values of the second-order approximations of the required concentrations can be determined using the standard relation shown in Equation (21) [28].

$$\alpha_{2\rho} = \frac{1}{\theta L_x L_y L_z} \int_0^\theta \int_0^{L_x} \int_0^{L_y} \int_0^{L_z} [\rho_2(x, y, z, t) - \rho_1(x, y, z, t)] dz dy dx dt \quad (21)$$

$$\begin{aligned}\alpha_{2C} = 0, \alpha_{2\phi l} = 0, \alpha_{2\phi V} = 0, \alpha_{2V} = \sqrt{\frac{(b_3+E)^2}{4b_4^2} - 4 \left( F + \frac{\theta a_3 F + \theta^2 L_x L_y L_z b_1}{b_4} \right)} - \frac{b_3+E}{4b_4}, \\ \alpha_{2l} = \frac{C_V - \alpha_{2V}^2 S_{VV00} - \alpha_{2V} (2S_{VV01} + S_{IV10} + \theta L_x L_y L_z) - S_{VV02} - S_{IV11}}{S_{IV01} + \alpha_{2V} S_{IV00}} \quad (22)\end{aligned}$$

where

$$\begin{aligned}b_4 &= \frac{1}{\theta L_x L_y L_z} S_{IV00}^2 S_{VV00} - \frac{1}{\theta L_x L_y L_z} S_{VV00}^2 S_{II00} \\ b_3 &= -\frac{S_{II00} S_{VV00}}{\theta L_x L_y L_z} (2S_{VV01} + S_{IV10} + \theta L_x L_y L_z) + \frac{S_{IV00} S_{VV00}}{\theta L_x L_y L_z} (S_{IV01} + 2S_{II10} + S_{IV01} + \theta L_x L_y L_z) + \frac{S_{IV00}^2}{\theta L_x L_y L_z} (2S_{VV01} + S_{IV10} + \theta L_x L_y L_z) \\ &\quad - \frac{S_{IV00}^2 S_{IV10}}{\theta^3 L_x^3 L_y^3 L_z^3} \\ b_2 &= \frac{S_{II00} S_{VV00}}{\theta L_x L_y L_z} (S_{VV02} + S_{IV11} + C_V) - (S_{IV10} - 2S_{VV01} + \theta L_x L_y \times L_z)^2 + \frac{S_{IV01} S_{VV00}}{\theta L_x L_y L_z} (\theta L_x L_y L_z + 2S_{II10} + S_{IV01}) \\ &\quad + \frac{S_{IV00}}{\theta L_x L_y L_z} (S_{IV01} + 2S_{II10} + 2S_{IV01} + \theta L_x L_y \times L_z) (2S_{VV01} + \theta L_x L_y L_z + S_{IV10}) - \frac{S_{IV00}^2}{\theta L_x L_y L_z} (C_V - S_{VV02} - S_{IV11}) \\ &\quad + \frac{C_I S_{IV00}^2}{\theta^2 L_x^2 L_y^2 L_z^2} - \frac{2S_{IV10}}{\theta L_x L_y L_z} \times S_{IV00} S_{IV01} \\ b_1 &= S_{II00} \frac{S_{IV11} + S_{VV02} + C_V}{\theta L_x L_y L_z} (2S_{VV01} + S_{IV10} + \theta L_x L_y L_z) + \frac{S_{IV01}}{\theta L_x L_y L_z} (\theta L_x L_y \times L_z + 2S_{II10} + S_{IV01}) (2S_{VV01} + S_{IV10} + \theta L_y L_z) \\ &\quad - \frac{S_{IV10} S_{IV01}^2}{\theta L_x L_y L_z} - \frac{S_{IV00}}{\theta L_x L_y L_z} (3S_{IV01} + 2S_{II10} + \theta L_x L_y L_z) (C_V - S_{VV02} - S_{IV11}) + 2C_I S_{IV00} S_{IV01} \\ b_0 &= \frac{S_{II00}}{\theta L_x L_y L_z} (S_{IV00} + S_{VV02})^2 - \frac{S_{IV01}}{L_x L_y L_z} \times \frac{1}{\theta} (\theta L_x L_y L_z + 2S_{II10} + S_{IV01}) (C_V - S_{VV02} - S_{IV11}) + 2C_I S_{IV01}^2 \\ &\quad - S_{IV01} \frac{C_V - S_{VV02} - S_{IV11}}{\theta L_x L_y L_z} \times \frac{1}{\theta} (\theta L_x L_y L_z + 2S_{II10} + S_{IV01}) (C_V - S_{VV02} - S_{IV11}) + 2C_I S_{IV01}^2 \\ &\quad - S_{IV01} \frac{C_V - S_{VV02} - S_{IV11}}{\theta L_x L_y L_z} \times S_{IV01} (\theta L_x L_y L_z + 2S_{II10} + S_{IV01}) \\ C_I &= \frac{\alpha_{1l} \alpha_{1V}}{\theta L_x L_y L_z} S_{IV00} + \frac{\alpha_{1l}^2 S_{II00}}{\theta L_x L_y L_z} - \frac{S_{II20} S_{II20}}{\theta L_x L_y L_z} - \frac{S_{IV11}}{\theta L_x L_y L_z} \\ C_V &= \alpha_{1l} \alpha_{1V} S_{IV00} + \alpha_{1V}^2 S_{VV00} - S_{VV02} - S_{IV11} \\ E &= \sqrt{8y + \theta^2 \frac{a_3^2}{a_4^2} - 4\theta \frac{a_2}{a_4}} \\ F &= \frac{\theta a_2}{6a_4} + \sqrt[3]{\sqrt{r^2 + s^3} - r} - \sqrt[3]{\sqrt{r^2 + s^3} + r} \\ r &= \frac{\theta^3 b_2}{24b_4^2} \left( 4b_0 - \theta L_x L_y L_z \frac{b_1 b_3}{b_4} \right) - \frac{\theta^3 b_3^2}{54b_4^3} - b_0 \frac{\theta^2}{8b_4^2} \times \left( 4\theta b_2 - \theta^2 \frac{b_3^2}{b_4} \right) - L_x^2 L_y^2 L_z^2 \frac{\theta^4 b_1^2}{8b_4^2} \\ s &= \theta^2 \frac{4b_0 b_4 - \theta L_x L_y L_z b_1 b_3}{12b_4^2} - \frac{\theta b_2}{18b_4}\end{aligned} \quad (22a)$$

Next, we determined the solutions of Equations (12a), (12b) and (12c), i.e. components of displacement vector. To determine the first-order approximations of these components using the method of averaging function corrections, we replaced the required functions on the right sides of the equations with their not yet known average

Substituting the relations from Equations (20a), (20b) and (20c) into Equation (21) allows us to obtain the required average values  $\alpha_{2\rho}$  as shown in Equations (22).

values  $\alpha_i$ . The substitution leads to the following result shown in Equation (23).

Integrating both sides of these relations over time  $t$  results in Equations (24).

$$\begin{aligned} \rho(z) \frac{\partial^2 u_{1x}(x, y, z, t)}{\partial t^2} &= -K(z)\beta(z) \frac{\partial T(x, y, z, t)}{\partial x} \\ \rho(z) \frac{\partial^2 u_{1y}(x, y, z, t)}{\partial t^2} &= \rho(z) \frac{\partial^2 u_{1y}(x, y, z, t)}{\partial t^2} \\ &= -K(z)\beta(z) \frac{\partial T(x, y, z, t)}{\partial y} \end{aligned} \quad (23)$$

$$\begin{aligned} \rho(z) \frac{\partial^2 u_{1z}(x, y, z, t)}{\partial t^2} &= -K(z)\beta(z) \frac{\partial T(x, y, z, t)}{\partial z} \\ u_{1x}(x, y, z, t) &= u_{0x} + K(z) \frac{\beta(z)}{\rho(z)} \frac{\partial}{\partial x} \int_0^t \int_0^\vartheta T(x, y, z, \tau) d\tau d\vartheta \\ &- K(z) \frac{\beta(z)}{\rho(z)} \frac{\partial}{\partial x} \int_0^\infty \int_0^\vartheta T(x, y, z, \tau) d\tau d\vartheta \end{aligned} \quad (24)$$

$$\begin{aligned} u_{1y}(x, y, z, t) &= u_{0y} + K(z) \frac{\beta(z)}{\rho(z)} \frac{\partial}{\partial y} \int_0^t \int_0^\vartheta T(x, y, z, \tau) d\tau d\vartheta \\ &- K(z) \frac{\beta(z)}{\rho(z)} \frac{\partial}{\partial y} \int_0^\infty \int_0^\vartheta T(x, y, z, \tau) d\tau d\vartheta \\ u_{1z}(x, y, z, t) &= u_{0z} + K(z) \frac{\beta(z)}{\rho(z)} \frac{\partial}{\partial z} \int_0^t \int_0^\vartheta T(x, y, z, \tau) d\tau d\vartheta \\ &- K(z) \frac{\beta(z)}{\rho(z)} \frac{\partial}{\partial z} \int_0^\infty \int_0^\vartheta T(x, y, z, \tau) d\tau d\vartheta \end{aligned}$$

Approximations of the second and higher orders of the components of the displacement vector can be determined using the standard method of replacing the required components with the sums  $\alpha_i + u_i(x, y, z, t)$  [28]. This replacement leads to the result shown in Equation (25).

$$\begin{aligned} \rho(z) \frac{\partial^2 u_{2x}(x, y, z, t)}{\partial t^2} &= \left\{ K(z) + \frac{5E(z)}{6[1 + \sigma(z)]} \right\} \frac{\partial^2 u_{1x}(x, y, z, t)}{\partial x^2} + \left\{ K(z) - \frac{E(z)}{3[1 + \sigma(z)]} \right\} \frac{\partial^2 u_{1y}(x, y, z, t)}{\partial x \partial y} + \frac{\partial^2 u_{1y}(x, y, z, t)}{\partial x \partial y} \\ &+ \frac{E(z)}{2[1 + \sigma(z)]} \left[ \frac{\partial^2 u_{1y}(x, y, z, t)}{\partial y^2} + \frac{\partial^2 u_{1z}(x, y, z, t)}{\partial z^2} \right] - \frac{\partial T(x, y, z, t)}{\partial x} \times K(z)\beta(z) \\ &+ \left\{ K(z) + \frac{E(z)}{3[1 + \sigma(z)]} \right\} \frac{\partial^2 u_{1z}(x, y, z, t)}{\partial x \partial z} \\ \rho(z) \frac{\partial^2 u_{2y}(x, y, z, t)}{\partial t^2} &= \frac{E(z)}{2[1 + \sigma(z)]} \left[ \frac{\partial^2 u_{1y}(x, y, z, t)}{\partial x^2} + \frac{\partial^2 u_{1x}(x, y, z, t)}{\partial x \partial y} \right] - \frac{\partial T(x, y, z, t)}{\partial y} \times K(z)\beta(z) \\ &+ \frac{\partial}{\partial z} \left\{ \frac{E(z)}{2[1 + \sigma(z)]} \left[ \frac{\partial u_{1y}(x, y, z, t)}{\partial z} + \frac{\partial u_{1z}(x, y, z, t)}{\partial y} \right] \right\} + \frac{\partial^2 u_{1y}(x, y, z, t)}{\partial y^2} \times \left\{ \frac{5E(z)}{12[1 + \sigma(z)]} + K(z) \right\} \\ &+ \left\{ K(z) - \frac{E(z)}{6[1 + \sigma(z)]} \right\} \frac{\partial^2 u_{1y}(x, y, z, t)}{\partial y \partial z} + K(z) \frac{\partial^2 u_{1y}(x, y, z, t)}{\partial x \partial y} \\ \rho(z) \frac{\partial^2 u_{2z}(x, y, z, t)}{\partial t^2} &= \frac{E(z)}{2[1 + \sigma(z)]} \left[ \frac{\partial^2 u_{1z}(x, y, z, t)}{\partial x^2} + \frac{\partial^2 u_{1z}(x, y, z, t)}{\partial y^2} + \frac{\partial^2 u_{1x}(x, y, z, t)}{\partial x \partial z} + \frac{\partial^2 u_{1y}(x, y, z, t)}{\partial y \partial z} \right] \\ &+ \frac{\partial}{\partial z} \left\{ K(z) \left[ \frac{\partial u_{1x}(x, y, z, t)}{\partial x} + \frac{\partial u_{1y}(x, y, z, t)}{\partial y} + \frac{\partial u_{1z}(x, y, z, t)}{\partial z} \right] \right\} \\ &+ \frac{E(z)}{6[1 + \sigma(z)]} \frac{\partial}{\partial z} \left[ 6 \frac{\partial u_{1z}(x, y, z, t)}{\partial z} - \frac{\partial u_{1x}(x, y, z, t)}{\partial x} - \frac{\partial u_{1y}(x, y, z, t)}{\partial y} \right. \\ &\left. - \frac{\partial u_{1z}(x, y, z, t)}{\partial z} \right] - \frac{\partial u_{1x}(x, y, z, t)}{\partial x} - \frac{\partial u_{1y}(x, y, z, t)}{\partial y} - \frac{\partial u_{1z}(x, y, z, t)}{\partial z} \left\} \frac{E(z)}{1 + \sigma(z)} - K(z)\beta(z) \frac{\partial T(x, y, z, t)}{\partial z} \right\} \end{aligned} \quad (25)$$

Integrating both sides of the above relations over time  $t$  leads to the results shown in Equation (26).

In this paper, we determined the concentrations of the dopant, the concentrations of radiation defects, and the components of the displacement vector using the second-order approximation within the framework of the method of averaging function corrections. This approximation is

typically sufficiently for qualitative analysis and allows for obtaining some quantitative results. All results obtained results were verified by comparison with numerical simulations.

$$\begin{aligned}
 u_{2x}(x, y, z, t) = & \frac{1}{\rho(z)} \left\{ K(z) + \frac{5E(z)}{6[1 + \sigma(z)]} \right\} \frac{\partial^2}{\partial x^2} \int_0^t \int_0^\vartheta u_{1x}(x, y, z, \tau) d\tau d\vartheta + \frac{1}{\rho(z)} \left\{ K(z) - \frac{E(z)}{3[1 + \sigma(z)]} \right\} \frac{\partial^2}{\partial x \partial y} \int_0^t \int_0^\vartheta u_{1y}(x, y, z, \tau) d\tau d\vartheta \\
 & + \frac{E(z)}{2\rho(z)} \left[ \frac{\partial^2}{\partial y^2} \int_0^t \int_0^\vartheta u_{1y}(x, y, z, \tau) d\tau d\vartheta + \frac{\partial^2}{\partial z^2} \int_0^t \int_0^\vartheta u_{1z}(x, y, z, \tau) d\tau d\vartheta \right] \frac{1}{1 + \sigma(z)} \\
 & + \frac{1}{\rho(z)} \frac{\partial^2}{\partial x \partial z} \int_0^t \int_0^\vartheta u_{1z}(x, y, z, \tau) d\tau d\vartheta \left\{ K(z) + \frac{E(z)}{3[1 + \sigma(z)]} \right\} - K(z) \frac{\beta(z)}{\rho(z)} \frac{\partial}{\partial x} \int_0^t \int_0^\vartheta T(x, y, z, \tau) d\tau d\vartheta \\
 & - \frac{\partial^2}{\partial x^2} \int_0^\infty \int_0^\vartheta u_{1x}(x, y, z, \tau) d\tau d\vartheta \times \frac{1}{\rho(z)} \left\{ K(z) + \frac{5E(z)}{6[1 + \sigma(z)]} \right\} \\
 & - \left\{ K(z) - \frac{E(z)}{3[1 + \sigma(z)]} \right\} \frac{\partial^2}{\partial x \partial y} \int_0^\infty \int_0^\vartheta u_{1y}(x, y, z, \tau) d\tau d\vartheta \times \frac{1}{\rho(z)} \\
 & - \frac{E(z)}{2\rho(z)[1 + \sigma(z)]} \left[ \frac{\partial^2}{\partial y^2} \int_0^\infty \int_0^\vartheta u_{1y}(x, y, z, \tau) d\tau d\vartheta + \frac{\partial^2}{\partial z^2} \int_0^\infty \int_0^\vartheta u_{1z}(x, y, z, \tau) d\tau d\vartheta \right] \\
 & - \frac{1}{\rho(z)} \left\{ K(z) + \frac{E(z)}{3[1 + \sigma(z)]} \right\} \frac{\partial^2}{\partial x \partial z} \int_0^\infty \int_0^\vartheta u_{1z}(x, y, z, \tau) d\tau d\vartheta + u_{0x} + K(z) \frac{\beta(z)}{\rho(z)} \times \frac{\partial}{\partial x} \int_0^\infty \int_0^\vartheta T(x, y, z, \tau) d\tau d\vartheta
 \end{aligned}$$

$$\begin{aligned}
 u_{2y}(x, y, z, t) = & \frac{E(z)}{2\rho(z)[1 + \sigma(z)]} \left[ \frac{\partial^2}{\partial x^2} \int_0^t \int_0^\vartheta u_{1x}(x, y, z, \tau) d\tau d\vartheta + \frac{\partial^2}{\partial x \partial y} \int_0^t \int_0^\vartheta u_{1x}(x, y, z, \tau) d\tau d\vartheta \right] \times \frac{1}{1 + \sigma(z)} \\
 & + \frac{K(z)}{\rho(z)} \frac{\partial^2}{\partial x \partial y} \int_0^t \int_0^\vartheta u_{1y}(x, y, z, \tau) d\tau d\vartheta + \frac{1}{\rho(z)} \left\{ \frac{5E(z)}{12[1 + \sigma(z)]} + K(z) \right\} \times \frac{\partial^2}{\partial y^2} \int_0^t \int_0^\vartheta u_{1x}(x, y, z, \tau) d\tau d\vartheta \\
 & + \frac{1}{2\rho(z)} \frac{\partial}{\partial z} \left\{ \frac{E(z)}{1 + \sigma(z)} \left[ \frac{\partial}{\partial z} \int_0^t \int_0^\vartheta u_{1y}(x, y, z, \tau) d\tau d\vartheta + \frac{\partial}{\partial y} \int_0^t \int_0^\vartheta u_{1z}(x, y, z, \tau) d\tau d\vartheta \right] \right\} \\
 & - K(z) \frac{\beta(z)}{\rho(z)} \int_0^t \int_0^\vartheta T(x, y, z, \tau) d\tau d\vartheta - \left\{ \frac{E(z)}{6[1 + \sigma(z)]} - K(z) \right\} \frac{1}{\rho(z)} \frac{\partial^2}{\partial y \partial z} \int_0^t \int_0^\vartheta u_{1y}(x, y, z, \tau) d\tau d\vartheta \\
 & - \frac{E(z)}{2\rho(z)} \left[ \frac{\partial^2}{\partial x^2} \int_0^\infty \int_0^\vartheta u_{1x}(x, y, z, \tau) d\tau d\vartheta + \frac{\partial^2}{\partial x \partial y} \int_0^\infty \int_0^\vartheta u_{1x}(x, y, z, \tau) d\tau d\vartheta \right] \frac{1}{1 + \sigma(z)} \\
 & - K(z) \frac{\beta(z)}{\rho(z)} \int_0^\infty \int_0^\vartheta T(x, y, z, \tau) d\tau d\vartheta - \frac{K(z)}{\rho(z)} \times \frac{\partial^2}{\partial x \partial y} \int_0^\infty \int_0^\vartheta u_{1y}(x, y, z, \tau) d\tau d\vartheta \\
 & - \frac{1}{\rho(z)} \frac{\partial^2}{\partial y^2} \int_0^\infty \int_0^\vartheta u_{1x}(x, y, z, \tau) d\tau d\vartheta \left\{ \frac{5E(z)}{12[1 + \sigma(z)]} + K(z) \right\} \\
 & - \frac{\partial}{\partial z} \left\{ \frac{E(z)}{1 + \sigma(z)} \left[ \frac{\partial}{\partial z} \int_0^\infty \int_0^\vartheta u_{1y}(x, y, z, \tau) d\tau d\vartheta + \frac{\partial}{\partial y} \int_0^\infty \int_0^\vartheta u_{1z}(x, y, z, \tau) d\tau d\vartheta \right] \right\} \times \frac{1}{2\rho(z)} \\
 & - \frac{1}{\rho(z)} \left\{ K(z) - \frac{E(z)}{6[1 + \sigma(z)]} \right\} \frac{\partial^2}{\partial y \partial z} \int_0^\infty \int_0^\vartheta u_{1y}(x, y, z, \tau) d\tau d\vartheta + u_{0y}
 \end{aligned} \tag{26}$$

$$\begin{aligned}
 u_z(x, y, z, t) = & \frac{E(z)}{2[1 + \sigma(z)]} \left[ \frac{\partial^2}{\partial x^2} \int_0^\infty \int_0^\vartheta u_{1z}(x, y, z, \tau) d\tau d\vartheta + \frac{\partial^2}{\partial y^2} \int_0^\infty \int_0^\vartheta u_{1z}(x, y, z, \tau) d\tau d\vartheta + \frac{\partial^2}{\partial x \partial z} \int_0^\infty \int_0^\vartheta u_{1x}(x, y, z, \tau) d\tau d\vartheta \right. \\
 & \left. + \frac{\partial^2}{\partial y \partial z} \int_0^\infty \int_0^\vartheta u_{1y}(x, y, z, \tau) d\tau d\vartheta \right] \frac{1}{\rho(z)} \\
 & + \frac{1}{\rho(z)} \times \frac{\partial}{\partial z} \left\{ K(z) \left[ \frac{\partial}{\partial x} \int_0^\infty \int_0^\vartheta u_{1x}(x, y, z, \tau) d\tau d\vartheta + \frac{\partial}{\partial y} \int_0^\infty \int_0^\vartheta u_{1x}(x, y, z, \tau) d\tau d\vartheta + \frac{\partial}{\partial z} \int_0^\infty \int_0^\vartheta u_{1x}(x, y, z, \tau) d\tau d\vartheta \right] \right\} \\
 & + \frac{1}{6\rho(z)} \frac{\partial}{\partial z} \left\{ \frac{E(z)}{1 + \sigma(z)} \left[ 6 \frac{\partial}{\partial z} \int_0^\infty \int_0^\vartheta u_{1z}(x, y, z, \tau) d\tau d\vartheta - \frac{\partial}{\partial x} \int_0^\infty \int_0^\vartheta u_{1x}(x, y, z, \tau) d\tau d\vartheta \right. \right. \\
 & \left. \left. - \frac{\partial}{\partial y} \int_0^\infty \int_0^\vartheta u_{1y}(x, y, z, \tau) d\tau d\vartheta - \frac{\partial}{\partial z} \int_0^\infty \int_0^\vartheta u_{1z}(x, y, z, \tau) d\tau d\vartheta \right] \right\} - K(z) \frac{\beta(z)}{\rho(z)} \frac{\partial}{\partial z} \int_0^\infty \int_0^\vartheta T(x, y, z, \tau) d\tau d\vartheta + u_{0z}
 \end{aligned}$$

### III. DISCUSSION

In this section we analyzed the dynamics of dopant redistributions and radiation defects during annealing, influenced by mismatch-induced stress and changes in porosity. Figures 2 and 3 present the typical distributions of concentration of dopant in heterostructures for diffusion and ion doping, respectively. These distributions were calculated under the condition where the value of dopant diffusion

coefficient in doped area is larger than in the nearest areas. The figures show that the inhomogeneity of the heterostructure allows for an increase in the compactness of dopants concentrations while simultaneously enhancing the homogeneity of dopant distribution within the doped part of the epitaxial layer. However, when manufacturing bipolar transistor using this approach, it is necessary to optimize the annealing of dopant and/or radiation defects. This optimization is necessary for the following reasons: if the annealing time is too short, the dopant will not reach the

interfaces between the materials of the heterostructure, resulting in no modifications to the distribution of the concentration of dopant. Conversely, if the annealing time is too long, the distribution of the concentration of dopant becomes too homogenous. We optimize the annealing time using a recently introduced approach. According to this criterion, we approximate the real distribution of the concentration of dopant with a stepwise function (see Figure 4 and 5). We then determine the optimal annealing time by minimizing the following mean-squared error,

$$U = \frac{1}{L_x L_y L_z} \int_0^{L_x} \int_0^{L_y} \int_0^{L_z} [C(x, y, z, \Theta) - \psi(x, y, z)] dz dy dx \quad (27)$$

where  $\psi(x, y, z)$  represents the approximation function. The dependencies of the optimal annealing time on various parameters are presented in Figures 6 and 7 for diffusion and ion doping, respectively. It is important to note that radiation defects must be annealed after ion implantation. During this annealing, the distribution of the concentration of dopant can spread. Ideally, the dopant distribution reaches the appropriate interfaces between the heterostructure materials during the annealing of radiation defects. If the dopant does not achieve these interfaces, additional annealing is required. In this case, the optimal additional annealing time for the implanted dopant is shorter than the annealing time for the infused dopant.

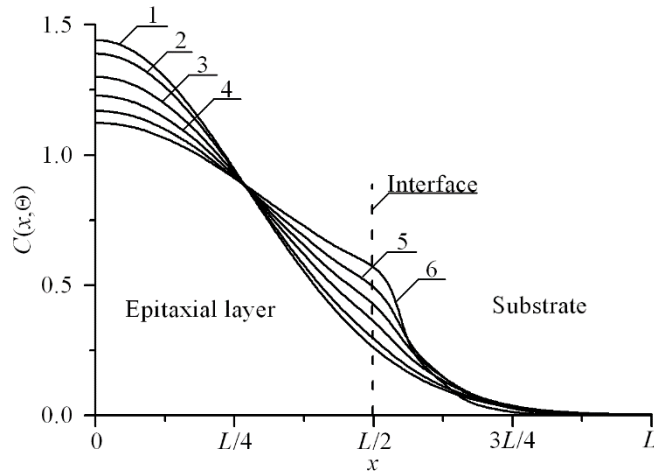


Figure 2. Distributions of the infused dopant concentration in the heterostructure from Figure 1 are shown in a direction perpendicular to the interface between the epitaxial layer substrates. An increasing number of curves correspond to a greater difference between the values of dopant diffusion coefficient in the layers of the heterostructure, with the value of dopant diffusion coefficient in epitaxial layer being larger than value of dopant diffusion coefficient in substrate.

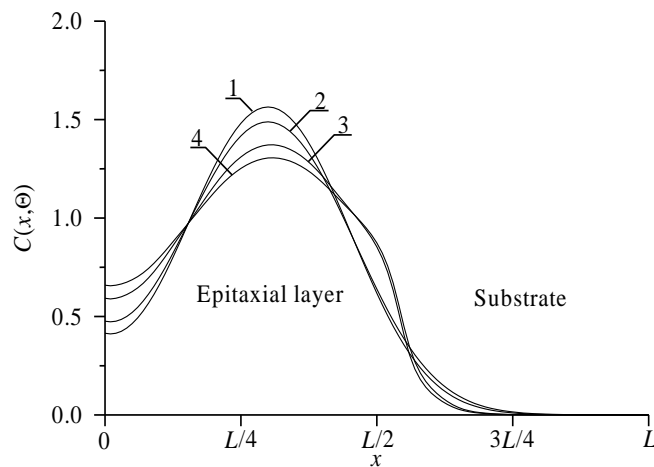


Figure 3. Distributions of the implanted dopant concentration in heterostructure from Figure 1 in a direction perpendicular to the interface between the epitaxial layer substrates. Curves 1 and 3 correspond to an annealing time  $\Theta = 0.0048(L_x^2 + L_y^2 + L_z^2)/D_0$ . Curves 2 and 4 correspond to an annealing time  $\Theta = 0.0057(L_x^2 + L_y^2 + L_z^2)/D_0$ . Curves 1 and 2 represent a homogenous sample. Curves 3 and 4 correspond to heterostructure where value of dopant diffusion coefficient in epitaxial layer is larger, than the value of dopant diffusion coefficient in the substrate.

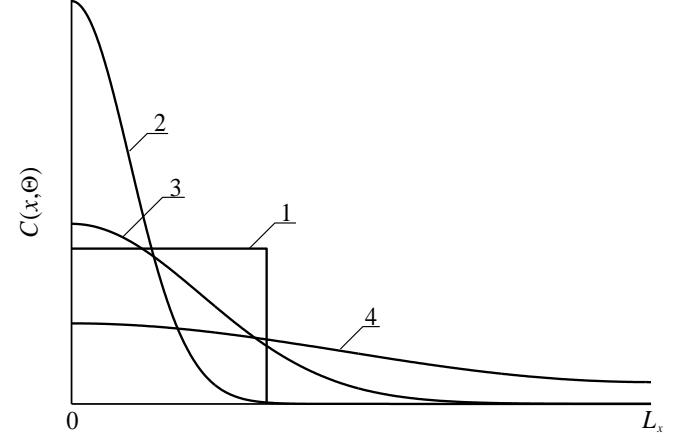


Figure 4. Spatial distributions of dopant in the heterostructure after dopant infusion. Curve 1 is the idealized distribution of dopant. Curves 2-4 are the real distributions of dopant for different values of annealing time. As the number of curves increases, the annealing time increases.

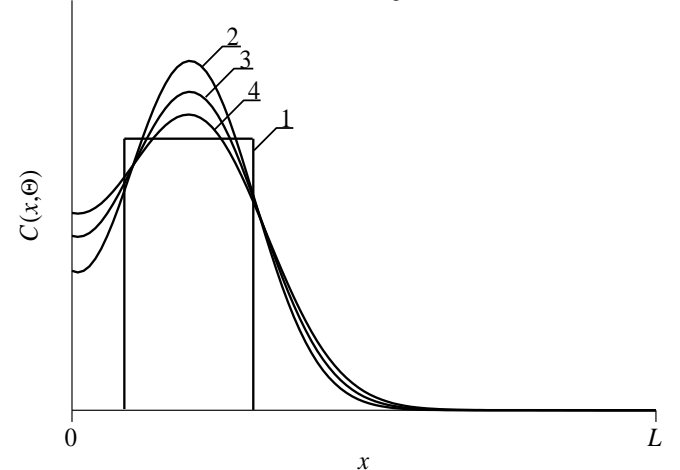


Figure 5. Spatial distributions of dopant in the heterostructure after ion implantation. Curve 1 is the idealized distribution of dopant. Curves 2-4 are the real distributions of dopant for varying values of annealing time. An increasing number of curves corresponds to a longer annealing time.

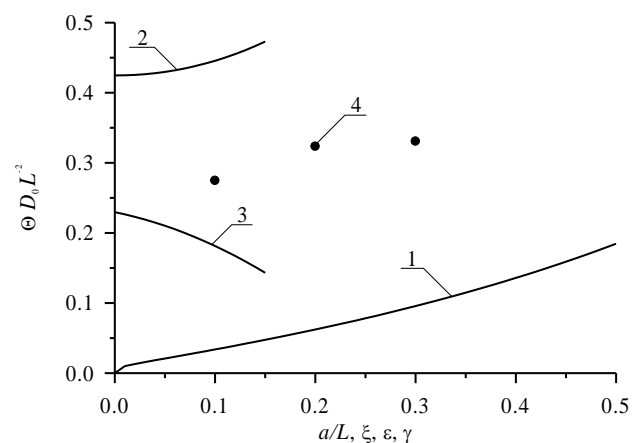


Figure 6. Dependence of dimensionless optimal annealing time for diffusion doping, obtained by minimizing the mean-squared error, on several parameters. Curve 1 is the dependence of dimensionless optimal annealing time on the relation  $a/L$  and  $\xi = \gamma = 0$  for equal values of the dopant diffusion coefficient in all parts of heterostructure. Curve 2 is the dependence of dimensionless optimal annealing time on the value of parameter  $\varepsilon$  for  $a/L=1/2$  and  $\xi = \gamma = 0$ . Curve 3 is the dependence of dimensionless optimal annealing time on the value of parameter  $\xi$  for

$a/L=1/2$  and  $\varepsilon = \gamma = 0$ . Curve 4 is the dependence of dimensionless optimal annealing time on the value of parameter  $\gamma$  for  $a/L=1/2$  and  $\varepsilon = \xi = 0$

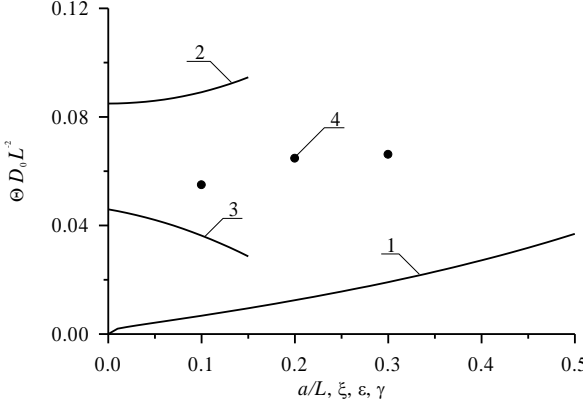


Figure 7. Dependences of dimensionless optimal annealing time for doping by ion implantation, obtained by minimizing the mean-squared error, on several parameters. Curve 1 is the dependence of dimensionless optimal annealing time on the relation  $a/L$  and  $\xi = \gamma = 0$  for equal values of the dopant diffusion coefficient in all parts of the heterostructure. Curve 2 is the dependence of dimensionless optimal annealing time on the value of parameter  $\varepsilon$  for  $a/L=1/2$  and  $\xi = \gamma = 0$ . Curve 3 is the dependence of dimensionless optimal annealing time on the value of parameter  $\xi$  for  $a/L=1/2$  and  $\varepsilon = \gamma = 0$ . Curve 4 is the dependence of dimensionless optimal annealing time on the value of parameter  $\gamma$  for  $a/L=1/2$  and  $\varepsilon = \xi = 0$ .

Next, we analyzed the influence of mechanical stress relaxation on the distribution of dopant in the doped areas of the heterostructure. Under the condition  $\varepsilon_0 < 0$ , compression of the dopant concentration distribution can be observed near the interface between the materials of the heterostructure. Conversely, for  $\varepsilon_0 > 0$ , spreading of the dopant concentration distribution occurs in this area. This change in dopant concentration can be at least partially compensated for by using laser annealing. Laser annealing allows for the acceleration of dopant diffusion and other processes in the annealed area due to the inhomogeneous temperature distribution and the Arrhenius law. Accounting for the relaxation of mismatch-induced stress in the heterostructure can lead to changes in the optimal annealing time. Additionally, modifying the porosity can decrease the mechanical stress. On the one hand, mismatch-induced stress can be used to increase the density of elements in integrated circuits. On the other hand, it can lead to a generation of dislocations due to discrepancies. Figures 8 and 9 show the distributions of vacancy concentration in porous materials and the component of the displacement vector perpendicular to the interface between layers of the heterostructure, respectively.

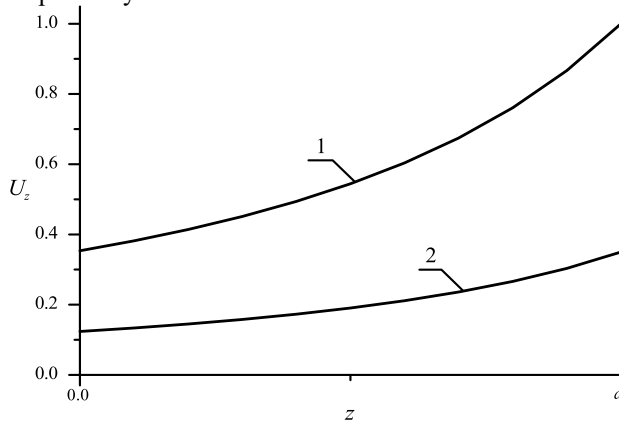


Figure 8. Normalized dependencies of the component  $u_z$  of the displacement vector on the coordinate  $z$  for nonporous (curve 1) and porous (curve 2) epitaxial layers.

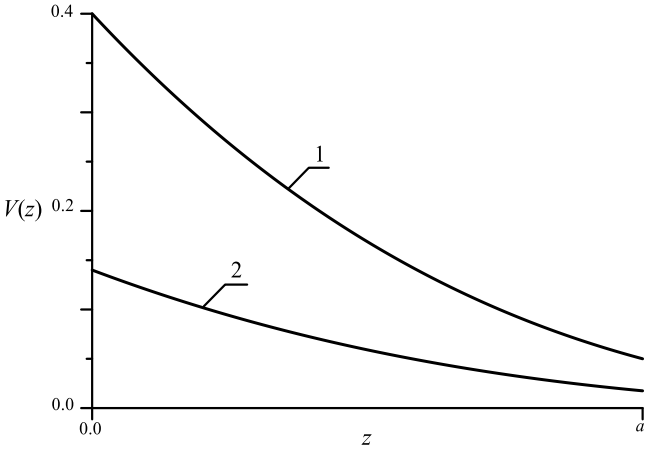


Figure 9. Normalized dependencies of vacancy concentrations on coordinate  $z$  in unstressed (curve 1) and stressed (curve 2) epitaxial layers.

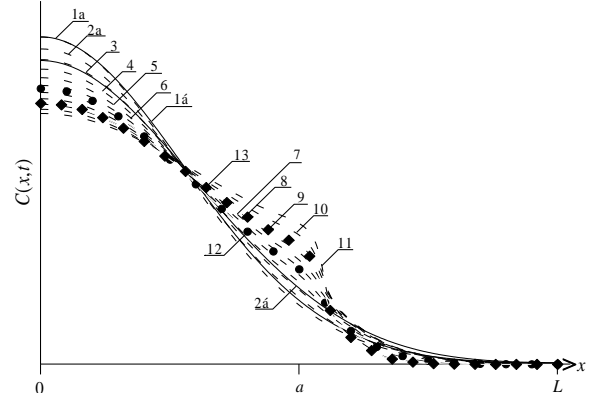


Figure 10. Spatial distributions of dopant in the system epitaxial layer - substrate at the same value of annealing time. Solid lines are the analytical calculation, while dashed lines are the numerical results. Curves 1-10 correspond to the normalized amplitude of variation of the dopant diffusion coefficient  $D = D_0[1 + \varepsilon g(x, T)]$ , where  $D_0$  is the average value of the dopant diffusion coefficient,  $0 \leq \varepsilon \leq 1$ ,  $|g(x, T)| \leq 1$ :  $\varepsilon = 0$ ;  $\varepsilon = 0.1$ ; ...;  $\varepsilon = 0.9$ ;  $\varepsilon = 0.999$ . Curves 11 and 12 correspond to experimental data from Ref. [28] (at  $\varepsilon = 0.62$ ) and Ref. [29] (at  $\varepsilon = 0.84$ )

#### IV. CONCLUSION

In this paper we model the redistribution of infused and implanted dopants, considering the relaxation mismatch-induced stress during the manufacturing of field-effect heterotransistors and heterodiodes within the framework of a double boost DC-DC converter. We provide recommendations for optimizing annealing to reduce the dimensions of transistors and to increase their density. We also offer suggestions to reduce mismatch-induced stress. An analytical approach to model diffusion and ion doping that considers the concurrent changing of parameters over space and time has been introduced. This approach allows us to consider the nonlinearity of the processes involved.

#### REFERENCES

- [1] H. -C. Chien, "Full-Phase Operation Transresistance-Mode Precision Full-Wave Rectifier Designs Using Single Operational Transresistance Amplifier", Active and Passive Electronic Components, vol. 2019, 2019.
- [2] S. Kundu, S. Sarkar, P. Mandal and A. Islam, "Modeling and sizing of non-linear CMOS analog circuits used in mixed signal systems", Analog Integrated Circuits and Signal Processing, vol. 99, no. 1, pp. 95-109, 2019.
- [3] G. Singh, M. H. Pasha, M. Shashidhar, and Z. Tabassum, "CMOS realization of OTRA based electronically controllable square wave

- generator enhancing linearity with minimum total harmonic distortion and power consumption”, International Journal of Innovative Research in Electronics and Communications, vol. 6, no. 1, pp 1-6, 2019.
- [4] E. M. Trukhanov, A. V. Kolesnikov, and I. D. Loshkarev, “Long-range stresses generated by misfit dislocations in epitaxial films”, Russian Microelectronics, vol. 44, no. 8, pp. 552-558, 2015.
- [5] B. -R. Lin, G. -H. Lin, and A. Jian, “An Agile VCO Frequency Calibration Technique for a 10-GHz CMOS PLL”, Electronics, vol. 8, no. 3, pp. 3-19, 2019.
- [6] V. Y. Stenin, and Y. V. Katunina, “Simulation the Effects of Single Nuclear Particles on STG RS Triggers with Transistors Spacing into Two Groups”, Russian Microelectronics, vol. 47, no. 6, pp. 407-414, 2018.
- [7] E. L. Pankratov, “About analysis of influence of radiation dose on charge carrier mobility value,” International Journal of Electrical and Data Communication, vol. 3, no. 1, pp. 33-40, 2022.
- [8] M. A. Al-Absi, E. S. Al-Suaibani, and M. T. Abuelmaatti, “A new CMOS current-mode controllable-gain square rooting circuit using MOSFET in subthreshold,” Analog Integrated Circuits and Signal Processing, vol. 90, pp. 431-434, 2017.
- [9] P. B. Petrovic, “Variable mode CMOS full-wave rectifier,” Analog Integrated Circuits and Signal Processing, vol. 90, pp. 659-668, 2017.
- [10] T. Jalilzadeh, M. T. Hagh, and M. Sabahi, “Analytical study and simulation of a transformer-less photovoltaic grid connected inverter with a delta-type tridirection clamping cell for leakage current elimination,” The International Journal for Computation and Mathematics in Electrical and Electronic Engineering, vol. 37, no. 2, pp. 814-831, 2018.
- [11] M. M. Lwin, “High-performance double boost dc-dc converter based on fuzzy logic controller”, Mechatronics and Applications: An International Journal, vol. 2, no. 1, pp. 1-12, 2018.
- [12] E. L. Pankratov, and E. A. Bulaeva, “Doping of materials during manufacture p-n-junctions and bipolar transistors. Analytical approaches to model technological approaches and ways of optimization of distributions of dopants”, Reviews in Theoretical Science, vol. 1, no. 1, pp. 58-82, 2013.
- [13] S. A. Kukushkin, A. V. Osipov, and A. I. Romanychev. “Epitaxial growth of zinc oxide by the method of atomic layer deposition on SiC/Si substrates”, Physics of the Solid State, vol. 58, no. 7, pp. 1448-1452, 2016.
- [14] E. M. Trukhanov, A. V. Kolesnikov, and I. D. Loshkarev, “Long-range stresses generated by misfit dislocations in epitaxial films”, Russian Microelectronics, vol. 44, no. 8, pp. 552-558, 2015.
- [15] E. L. Pankratov, and E. A. Bulaeva, “On optimization of regimes of epitaxy from gas phase. some analytical approaches to model physical processes in reactors for epitaxy from gas phase during growth films”, Reviews in Theoretical Science, vol. 3, no. 4, pp. 365-398, 2015.
- [16] K. K. Ong, K. L. Pey, P. S. Lee, A. T. S. Wee, X. C. Wang, and Y. F. Chong, “Dopant activation in subamorphized silicon upon laser annealing”, Appl. Phys. Lett., vol. 89, no. 17, pp. 172111-172114, 2006.
- [17] H. T. Wang, L. S. Tan, and E. F. Chor, “Pulsed laser annealing of Be-implanted GaN”, J. Appl. Phys., vol. 98, no. 9, pp. 094901-094905, 2006.
- [18] Y. V. Bykov, A. G. Yeremeev, N. A. Zharova, I. V. Plotnikov, K. I. Rybakov, M. N. Drozdov, Y. N. Drozdov, and V. D. Skupov, “Diffusion Processes in Semiconductor Structures During Microwave Annealing”, Radiophysics and Quantum Electronics, vol. 43, no. 3, pp. 836-843, 2003.
- [19] Y. W. Zhang, and A. F. Bower, Journal of the Mechanics and Physics of Solids, vol. 47, no. 11, pp. 2273-2297, 1999.
- [20] L. D. Landau, and E. M. Lifshits, in Theoretical of Elasticity: Volume 7 (Theoretical Physics), Phymatlit, Moscow, 2001.
- [21] M. Kitayama, T. Narushima, W. C. Carter, R. M. Cannon, A. M. Glaeser, J. A. Ceram. Soc. “The Wulff shape of alumina: I, modeling the kinetics of morphological evolution”, Vol. 83, pp. 2561 (2000);
- [22] M. Kitayama, T. Narushima, A. M. Glaeser, J. A. Ceram. Soc. “The Wulff shape of Alumina: II, experimental measurements of pore shape evolution rates”, Vol. 83, pp. 2561 (2000);
- [23] P. G. Cheremskoy, V. V. Slesov, and V. I. Betekhtin, in Pore in Solid Bodies, Energoatomizdat, Moscow, 1990.
- [24] Z. Y. Gotra, “Technology of microelectronic devices,” in Radio and Communication, Moscow, 1991.
- [25] P. M. Fahey, P. B. Griffin, and J. D. Plummer, “Point defects and dopant diffusion in silicon”, Rev. Mod. Phys., vol. 61, no. 2, pp. 289-388, 1989.
- [26] V. L. Vinetskiy, and G. A. Kholodar', in Radiative Physics of Semiconductors, Kiev: Naukova Dumka, 1979.
- [27] M. G. Mynbaeva, E. N. Mokhov, A. A. Lavrent'ev, and K. D. Mynbaev, “High-temperature diffusion doping of porous silicon carbide”, Techn. Phys. Lett., vol. 34, no. 17, pp. 13, 2008.
- [28] Y. D. Sokolov, “About the definition of dynamic forces in the mine lifting”, Applied Mechanics, vol. 1, no. 1, pp. 23-35, 1955.
- [29] O. V. Alexandrov, “Modeling the concentration dependence of boron in silicon,” Semiconductors, vol. 38, no. 3, pp. 258-261, 2004.
- [30] N. T. Bagraev, L. E. Klyachkin, A. M. Malyarenko, A. I. Ryskin, and A. S. Shcheulin, “Heterojunctions p<sup>+</sup>-Si-n-CdF<sub>2</sub>,” Semiconductors, vol. 39, no. 5, pp. 528-532, 2005.